AUTHOR COMMENTS

GENERAL COMMENTS

The authors would like to thank the three anonymous referees for their helpful comments and suggestions. We have addressed all comments which we believe significantly improved the revised manuscript. **A marked-up version of the manuscript is appended to the end of this response file.**

Two main concerns raised by the referees were (1) the effect of losses of semi-volatile vapors to the Teflon® chamber walls on our data and their implications and (2) that the implications of our work to the atmosphere were not clear in the original version of the manuscript. We address these main concerns here and address the more detailed comments below.

(1) Losses of semi-volatile vapors to the chamber walls

We agree with the Referees that wall losses of semi-volatile species occur in environmental chambers such as the chamber used for this work, and we have added a discussion of these losses in the revised manuscript. The challenges resulting from these losses are not unique to our study but rather apply to all environmental chamber experiments. Currently, losses of semi-volatile species are poorly constrained, and there is no consensus on how to accurately account for them.

In all of the experiments described here, the condensation sink after particle formation was approximately 1/min, while the initial condensation sink to ammonium sulfate seeds in seeded experiments ranged between 0.6 and 1/min. The timescale for sulfuric acid vapor wall loss in the Carnegie Mellon chamber is approximately 0.1/min, as determined by chemical ionization mass spectrometer measurement of sulfuric acid loss (V. Hofbauer, personal communication). Thus, in all of the seeded experiments, condensing vapors encountered the seeds approximately 10 times before encountering the walls, while in nucleation experiments the suspended aerosol population quickly grew to a size where this was also true. Thus, while wall losses of semi-volatile vapors are a source of uncertainty, we have attempted to ensure that vapor-particle interactions at least dominate over vapor-wall interactions. It is therefore reasonable to expect that observed differences between experiments are not driven by interactions with the walls but instead by chemical processing of the organic aerosol.

(2) Implications of work to the atmosphere

We have modified the discussion and the conclusion section to more specifically offer conclusions and atmospheric implications of this work. Uncertainties remain and underline the need for additional studies, but our results do offer new insights as well as directions for future study. Contributions and implications of our work include:

- Confirmation that photochemical aging influences SOA, as evidenced by the observed relationship between exposure to OH and physicochemical properties of SOA formed from the oxidation of toluene and other small aromatic VOCs
- A measured relationship between changes in organic aerosol (OA) oxidation state and saturation vapor pressure

- A measured relationship between changes in (OA) oxidation state and hygroscopicity. We found that there is no significant correlation between oxidation state and hygroscopity, which is an important result and suggests that both properties need to be measured to more fully characterize the OA.

SPECIFIC COMMENTS

All referee comments are addressed below. Referee comments are included in italics; author responses are written in plain text.

Referee 1

(1) *It isn't clear what new scientific knowledge this paper adds to the literature and it is less clear what the implications of this work are for the atmosphere. The manuscript would be greatly improved if the authors can offer more definitive and clear conclusions and discuss what the atmospheric implications of this work are.*

This has been addressed in the revised manuscript and in the response to general comment (2) above.

(2) *The authors do not discuss irreversible wall loss of semi-volatile species, which has been shown to be substantial and important for this (and many other) chemical system. … Other researchers have also concluded that faster chemistry (i.e., higher OH exposure) helps to minimize wall loss (e.g. (Kroll et al., 2007)) and that lower-volatility, more highly oxidized species are more likely to be lost (Matsunaga and Ziemann, 2010). Therefore, it seems plausible that the entirety of section 3.2 could/should be explained by variable wall loss driven by the different oxidation conditions. Figure 4 strongly suggests these effects, with lower yields found at similar aerosol mass loadings for the slower reacting, lower OH exposure experiment. Furthermore, the difficulty the researchers report in reproducing their observations during experiment designed to have identical oxidizing conditions (p 31458, second paragraph) suggests that wall loss is a contributing factor (probably the driving factor) to their measurements in these two experiments.*

As explained in our general comment (1) above it is reasonable to expect that observed differences between experiments are not driven by interactions with the walls but instead by chemical processing of the organic aerosol. We disagree with the Referee that the entirety of section 3.2 could be explained by variable wall loss driven by the oxidation conditions, and that Figure 4 strongly suggests this. To review, Expt. 7 is the lower OH exposure experiment and showed lower mass yields, a lower extent of oxidation and more volatile organic aerosol compared to Expt. 9. We note that the exposure to UV and OH in Expt. 7 (and therefore the time during which organic aerosol was formed) was only 10 minutes long, compared to 3 hours in Exp. 9. Thus, the time available for wall losses is much higher during Expt. 9 than during Expt. 7, and yet the OA mass

yields for Expt. 9 are higher than the yields for Expt. 7. Furthermore, if more highly oxidized species are more likely to be lost, Expt. 9 would be more strongly affected by wall losses. In summary, while there is one effect (slower reactions) that may increase wall losses in Expt. 7 compared to Expt. 9, there are two effects (time of OA formation and extent of oxidation of products formed) that would increase wall losses in Expt. 9 compared to Expt. 7. Thus, overall we do not expect wall losses to be higher in Expt. 7 compared to Expt. 9, and it is reasonable to assume that differences in the aerosol mass yields shown in Figure 4 are primarily due to differences in photochemical conditions.

Furthermore, our difficulty in repeating experiments with identical oxidizing conditions stemmed from our method of HONO injection, which we have found was not reproducible. We have since fixed this issue and are now using a more reproducible method of injection. Thus we believe that the different experiments designed to have the same oxidizing conditions actually had different oxidizing conditions because some HONO injections resulted in little or no HONO actually injected into the chamber.

(3) *The Materials and Methods section of the paper should be significantly shortened with much of the material either left out altogether or moved to the supplementary material*

We have moved a significant amount of material from the main manuscript to the supplementary material.

Technical and Editorial Comments

(4) *Title: Since the author don't separate aging from SOA formation and acknowledge this in the manuscript, shouldn't the title be changed to reflect this fact?*

We have modified the title. The revised title now reads "Formation and Aging of Secondary Organic Aerosol from Toluene: Changes in Chemical Composition, Volatility and Hygroscopicity"

(5) *P 31455, Lines 3-5. It seems very unlikely that the mean carbon oxidations state is three, 20 minutes into the experiment. This would require approximately 10 oxygen atoms being added to the molecule in 20 minutes. The authors should remove this statement from the manuscript or justify how this could be possible. It seems more likely that the unreasonably high oxidation state is a result of low S/N or some other artifact.*

Upon careful reconsideration of the data we have determined that this high initial oxidation state was indeed an artifact. First, we had made a mathematical error in calculating oxidation state from O:C and H:C values. Second, a small amount of background organic signal (equivalent to approximately 0.2 $\mu g/m^3$ see next comment) with very high oxidation state caused this high initial oxidation state. After subtracting the effects of this background organic aerosol on the oxidation state measurement, the oxidation state of the toluene SOA is approximately constant throughout the experiment as shown in the updated top panel of Figure 2. We have also updated

the values of oxidation state in Table 1 and in the analysis of volatility and hygroscopicity for this experiment (Figures 9 and 10), as well as the associated discussion. Organic aerosol data from the other experiments did not suffer from this background.

(6) *Figure 2, Experiment 2 panel: It appears that the organic aerosol concentration at the beginning of the experiment is not zero. Please comment on the source of the background aerosol.*

The small amount of organic aerosol (~0.2 $\mu g/m^3$) was also present on that day when a particle filter was connected to the inlet of the HR-AMS; it therefore appears to be an instrument artifact. According to the HR-AMS data analysis the oxidation state of the background organic signal is approximately 2. It could therefore be due to material of very low vapor pressure slowly vaporizing from the HR-AMS heater - organic material that does not flash-vaporize at 600°C.

(7) *P31455, lines 14-16 and 23-24. There is a contradiction here or else the message the authors are trying to convey is unclear. Lines 14-16 say that the aerosol oxidation state increased in experiment 9 and in all other experiments. A few lines later, experiment 3 is discussed and the oxidation state decreases during the experiment. Please correct this.*

We clarified this in the revised manuscript: In experiment 3 the oxidation state increases initially but decreases during the long overnight irradiation period.

(8) *Figure 8. I recommend moving this figure to the supplemental material. It isn't discussed in the text, is only mentioned in one sentence, and only shows the fitting routine is adequate.*

We have moved this figure to the supplemental material as suggested by the referee.

(9) *Figure 9. The trendline seems to be driven to a large extent by the single point at the upper left in the graph. How confident are the authors in this point? Without it, it appears that the fit would produce a very different slope and therefore conclusion.*

The oxidation state of the point at the upper left was influenced by background organic signal as explained in the response to comments (5) and (6) above. Upon correcting the data for this background signal the data point moved down (to lower oxidation state). This datapoint now does not anymore drive the trendline: including the point results in a slope of 0.28; removing the point results in a slope of 0.31. Thus, we conclude that a change in the oxidation state of about 0.3 units results in a change in volatility of about one order of magnitude.

Referee 2:

AMS analysis:

(1) *They attribute all NO/NO2 observed in AMS to organic nitrate since "no inorganic nitrate is added to or expected to be formed" (Page 31448, line 20). However, they add HONO which is photolyzed to NO, which is oxidized to NO2 and further to HNO3. The observed ratio of NO/NO2 = 8 is not a unique indicator for organic nitrate. This ratio varies from AMS to AMS and depends on the structure of ON. It has to be compared to the one recorded during their calibration using NH4NO3.*

The NO/NO2 ratio measured during calibrations using NH4NO3 is 2.4. This implies that the HNO3 formed in these experiments does not partition appreciably to the (neutral) aerosol present in these experiments, consistent with its high vapor pressure. We have added this information to the revised manuscript. That section now reads:

"Third, ions assigned to the nitrate family in the HR analysis (NO^+, NO_2^+) were added to the total organic aerosol mass in the HR batch table because they appear to be due to organic nitrates: The ratio of NO^+ to NO_2^+ measured in these experiments (Table 2) is around 8, much higher than the ratio of 2.4 measured in calibration experiments using ammonium nitrate. Furthermore, no inorganic nitrate was added in these experiments. Nitric acid is expected to form in the gas phase but does not appear to partition appreciably to the particle phase, consistent with its high vapor pressure (Fry et al., 2009)."

(2) *The measured O:C are rather high for the rather low OH exposures. The H:C seems to be very high, in some cases higher than 2 (exp 3, 9). The precursor toluene has a H:C of 1.14. Where does all that hydrogen come from? Could it be a problem of the AMS analysis?*

The AMS analysis in this manuscript is non-standard in that it determines the amount of H_2O^+ attributed to organics so that the mass of water does not correlate with the mass of organics ($R < 0.01$) as expected for these low relative humidity experiments. The ratios of organic H_2O^+ to $(^{13}CO_2^+ + CO_2^+)$ are provided in Table 2 and ranged from 0.3 to 2.4, higher than the ratio of 0.225 in the default fragmentation table but consistent with recent calibration experiments (Canagaratna et al., 2015). This results in higher O:C and H:C ratios than when using the standard constant factor.

Hydrogen atoms can be added to the carbon backbone in these experiments through OH addition or by the reaction of HO_2 and RO_2 producing peroxides. Considering that O:C values were near 1, even a doubling of the H:C ratio of the precursor molecule is possible.

(3) *They conclude that "the methyl carbon atom is about three times less likely than the aromatic carbon atoms to form organic acids" (page 31462, line 11). Can they show from seeded blank experiments that there is no background formation of SOA producing CO2 from 12C?*

Small concentrations of background organic signal such as was discovered to be present during experiment 2 could influence this result. Furthermore, as noted by Referee 3 not all CO_2^+ is necessarily due to organic acids. Due to these complications we have decided to remove these data and associated discussion from the revised manuscript.

(4) *Experiment 2 shows extremely high OSc in the beginning. These values (~3) are unbelievable even considering the multiperoxide formation mechanism recently reported. This experiment is reported with the highest OSc and defines basically the correlation between OSc and volatility (Fig. 9). All other points would yield a different dependence. How sure are the authors about the analysis of experiment 2. In Table 2 the OSc is given as 0.45. From Figure 2 it seems to be even higher and in Figure 10 it is shown as -0.2. It is also puzzling to see in Table 2 that the H2O/CO2 is completely different from all the other experiments. Is this real or an issue of data analysis? Figure 2 indicates a background aerosol. How much does this influence the result?*

The high OS_c at the beginning of experiment 2 was the result of an artifact related to the background aerosol as explained in the response to Comment 5 of Referee 1. We have corrected the data, all Figures and associated discussion in the revised manuscript.

(5) *Although not being an AMS specialist I wonder why the collection efficiency is so low (0.25), even for organics?*

AMS collection efficiency (CE) can differ between instruments and is still subject of active research. Recent work at Carnegie Mellon suggests a collection efficiency of organics of 0.3 (E. Robinson et al., in preparation). We also note that our collection efficiency estimation, since it is based on comparison of data from another instrument, could potentially account and correct for factors other than particle bounce at the vaporizer, for example the estimated ionization efficiency. The discussion of CE has been moved to the supplemental material in response to Referee #1.

Other:

(6) *They do not find a general correlation between OSc and hygroscopicity as was found by others. Thus they speculate on surfactants playing a role. I assume that kappa was calculated using ZSR for the mixed aerosols. As mentioned above, the aerosol might also contain inorganic nitrate which is not considered here and could explain observations.*

As mentioned in response to the Comment 1 above, our AMS data do not provide evidence for the presence of inorganic nitrate. Hence we have not changed this discussion in the revised version of our manuscript. We also note that while a number of other studies have found a link between OS_c and hygroscopicity, our study is not unique in not having found a clear correlation.

(7) *In the conclusions the authors state "experiments with higher OH exposure showed higher SOA mass yields". This is shown for exactly 2 experiments.*

In the conclusions of the revised manuscript we have clarified that this was only shown for 2 experiments. We have also removed "mass yields" from the title of the manuscript to reflect that the focus of this manuscript was not on SOA mass yields. Nevertheless, we choose to report the SOA mass yields for the two experiments (Expts. 7 and 9) for which these data are available.

(8) *Two experiments were performed with other aromatics as seen in Table 1. No other information is given in the manuscript.*

Additional discussion of these experiments has been added to the revised manuscript. Organic aerosol formed in experiments which included VOCs other than toluene did not exhibit significantly different properties (specifically, volatility and hygroscopicity), suggesting that other small aromatic VOCs appear to behave similarly as toluene. The choice of using toluene as a "model system" therefore appears appropriate.

Technical comments

(9) *P31450, line 15: here density is fixed to 1.5 gcm-3. In table S1 other densities are reported.*

We used the estimated densities (from Table S1) to convert between mobility diameter and aerodynamic diameter. What we intended to emphasize in this line is that the CE / density optimization routine is much less sensitive to density than to CE (and that CE does not change significantly when fixing density at 1.5). This discussion has been clarified and moved to the supplemental information in the revised manuscript.

P31456, line 20: the ratio would be 1/7

(10) We have removed these data from the revised manuscript.

(11) *P31457, line 2: Light is reported at 100% in Table 1 for all four experiments. Therefore there is not lower UV intensity.*

There was a typographical error in Table 1; only 1/3 of the lights were used in Experiment 7. This was corrected in the revised manuscript.

(12) *P31459, line 6: Table 1 reports 100% UV lights Table 1: correct units for OH exposure*

There was a typographical error in Table 1; only 1/3 of the lights were used in Experiment 7. This was corrected in the revised manuscript. The units for OH exposure were also corrected in the revised manuscript.

(13) *Figure 4: correct numbers for OH exposure*

This was corrected in the revised manuscript.

Referee 3:

(1) *Why was toluene (the only aromatic studied in any detail) chosen for these experiments? Is there something about the chemistry that makes it an interesting and important choice?*

Toluene is frequently used as a model system to study organic aerosol formation from small aromatic VOCs (Seinfeld and Pandis, 2006).

(2) *Page 31450, Second paragraph: How does OA density compare with values calculated using the parameterization developed by Kuwata et al. (2012), ES&T, 46, 787? This is a useful way of checking for significant errors.*

The OA density values agree reasonably well. The average density (averaged over all experiments) predicted using the parameterization developed by Kuwata et al. (2012) is 1.42, while the average density predicted using the Kostenidou et al. (2007) algorithm is 1.34. For nine out of the eight experiments, the density predictions differ by less than 10%; for experiment 2 the density predictions differ by 16%. In the analysis presented by Kuwata et al., their parameterization "has an accuracy of 12% for more than 90% of the 31 atmospherically relevant compounds used in the training set". Thus, the densities predicted by these different algorithms appear to agree within the uncertainties of the algorithms.

(3) *Page 31450, bottom paragraph: The approach for correcting for vapor loss to walls ignores the uptake into the Teflon film walls, which has been shown recently to be significant. Zhang et al. (2014) PNAS, 111, 5802 have shown that vapor wall losses in studies of SOA formation from toluene oxidation lead to underestimates in SOA yields by factors of 2–4. This issue should be discussed here and its potential effects on results, such as SOA mass, O/C ratios (loss of oxidized products to the walls that prevents further aging), etc.*

We acknowledge that wall losses are important, and a discussion of these effects has been added to the revised manuscript and is provided in our general comment (1). As also discussed in our general comment wall losses do not appear to dominate effects observed in these experiments.

(4) *Page 31453, first paragraph: This is the first I have heard of "shifting factors" and imagine this will be the case for many other readers. It would help to give the reader a feeling for what a certain relative reduction in "volatility" (an imprecise term) means in this framework. Is it somehow related to a relative change in average SOA vapor pressure or saturation concentration? Without this insight it is difficult to know if these represent large or small changes in "volatility".*

A shifting factor of 10 implies a reduction in the SOA saturation mass concentrations of 1 order of magnitude. This clarification has been added to the revised manuscript.

(5) *Page 31455, whole page: There is no discussion of the observation that SOA was higher with seed than without. Why? According to the PNAS paper referenced in Comment 3, this is likely due to reduced wall loss of vapors, which will affect the interpretation of SOA results and O/C ratios. I suggest discussing this.*

We only have data on precursor concentrations for experiments 7, 8 and 9, all of which were seeded experiments. We therefore cannot compute aerosol mass yields for the unseeded experiments and cannot compare yields in seeded and unseeded experiments. While the amount of organic aerosol formed is higher for the seeded than the unseeded experiment shown in Figure 2, this could be due to factors other than the seed effect, most notably a difference in the amount of toluene reacted.

(6) *Page 31455, bottom line: What compounds are expected to photolyze at significant rates in these experiments?*

Peroxides, which can form from photo-oxidation of volatile organic compounds (VOCs) have been shown to photolyze under similar conditions (Surratt et al., 2006). A reference regarding this has been added to the revised manuscript.

(7) *Figures 2 and 3. I suggest adding toluene time profiles to these figures so that one can determine the extent to which early-generation products are still being formed vs. more aged products. These profiles should also be discussed along with the other quantities.*

The toluene time series has been added to the bottom panel of Fig 2 of the revised manuscript (Expt. 9), and a discussion has been added to the text. Toluene data were not available during Expts. 2 (Figure 2, top panel) and 3 (Figure 3).

(8) *Page 31456, lines 20-25: I am not aware of a mechanism for forming organic acids under the high NOx conditions of these experiments. Please provide a reference of definitive evidence by others that acids are formed. Might the CO2+ ion instead come from acylperoxynitrates (PAN-type compounds with formula R–C(O)OO–NO2) formed by oxidation of aldehydes, which are well established products of toluene oxidation, in the presence of NO2? See Chan et al. (2010), ACP, 10, 7169. This would be consistent with the large nitrate content of the SOA.*

It is generally observed that organic acids, especially diacids, show very high CO_2^+ (Canagaratna et al., 2015). However, the point is well taken that organic acids are not the sole source of CO_2^+ after electron-impact ionization of 600°C aerosol vapors. A counter-indication to peroxyacylnitrates as dominant source of the observed CO_2^+ is that the "nitrate" (NO^+ and NO_2^+) signal in the SOA mass spectra was relatively volatile while the CO_2^+ signal was not. For example, when heating and evaporating the SOA formed in Expt. 9 at 100°C in the TD, the fraction of the total organic signal due to "nitrate" (NO^+ and NO_2^+) decreased by a factor of 3 while the fraction of the total organic signal due to CO_2^+ increased by approximately 40 percent.

(9) *Page 31457, lines 14-22: The Chan et al. (2010) reference given in Comment 8 indicates that for systems that form significant aldehydes, such as the one studied here, that SOA yields increase with increasing NO2/NO ratio. This is worth including in this discussion.*

During experiments with multiple HONO injections the concentrations of NO_x in the system exceeded the maximum calibrated concentration of the NO_x monitor (1 ppm). In addition, interference from organic nitrates, HONO and HNO_3 would complicate the quantification of NO_2 concentrations in this system. Thus, NO_x concentrations are not discussed in detail in this manuscript.

(10) *Page 457, bottom paragraph: With regards to acylperoxynitrates, it might be mentioned that they might still be mostly stable in the TD for the 15 s residence time. Thermal decomposition lifetimes range from about 20 min to 5 s for temperatures 40–100 C [Orlando and Tyndall (2012), Chem. Soc. Rev., 41, 6294].*

In the AMS, organic molecules are fragmented during flash vaporization and/or due to harsh electron impact ionization. Therefore, we are unable to determine the molecular identity of particle-phase organics and cannot comment on the presence of acylperoxynitrates in our experiments, nor their behavior in the thermodenuder.

(11) *Page 31459, lines 15–20. My recollection is that past TD measurements/modeling by the CMU group has indicated a mass accommodation coefficient for SOA of 0.01. Any idea what is so different here?*

Some modeling work has shown solutions for mass accommodation coefficients as low as 0.01 (Epstein et al., 2010) with relatively high enthalpy of vaporization based on a-priori assumptions but also a volatility distribution that we now know omits extremely low volatility organic carbon (ELVOC) in the SOA. A challenge in this modeling is always covariance between parameters such as accommodation coefficients and volatility, which both influence the kinetics of evaporation. However, experiments designed to isolate mass accommodation through equilibration timescale measurement (Saleh et al., 2013) consistently find mass accommodation coefficients exceeding 0.1.

(12) *Page 31460, lines 14–21: Can anything be said about what this 0.5 unit reduction in volatility corresponds to with regards to vapor pressure, and what the change corresponds to in carbon number or functional group composition (e.g., using the SIMPOL method)?*

The equation indicates that a reduction of 0.5 units of oxidation state is associated with an increase in saturation vapor pressure of 1 order of magnitude. Thus, the equation directly relates a change in functional group composition (as well as it can be estimated from AMS data on OA oxidation state) to a change in SOA saturation vapor pressure. We have added to this discussion in the text in order to clarify this point. In addition, a correction in the data analysis has changed the slope to 0.3, so indeed a reduction of 0.3 units of oxidation state is associated with an increase in vapor pressure (saturation mass concentration) of one order of magnitude.

(13) *Page 31461, bottom paragraph: What about the possibility that carbon chain length affects CCN activity? This is not accounted for in O/C ratio and oligomers eventually reach a solubility limit.*

We thank the referee for pointing out this possibility. We have included a discussion of this in the revised manuscript.

(14) *Page 31462, line 2: The attempt to generalize these results to "small aromatic VOCs" seems inappropriate, since although a few are listed in Table 1 as being added to toluene in 2 experiments, and there is no discussion of what effects they had, if any. In the absence of such results and discussion I suggest limiting the conclusions to toluene, with perhaps some comments on whether there is reason to believe that other small aromatics might behave similarly or differently and why. I also suggest changing the title from "small aromatic VOCs" to "toluene" for the same reasons.*

In the revised manuscript we have changed the title as suggested by the referee and focused our conclusions on toluene, while also commenting that other small aromatics appear to behave similarly.

(15) *Page 31462, Conclusions: It is stated in the Introduction: "A main objective is to connect the extent of oxidation and the changes in volatility of these experiments with the 2D-VBS framework." Was that objective met satisfactorily? How do these results contribute to broader objectives? Do these results help to explain what anyone else has observed, or are they specific to this study?*

The equation given in section 3.3.1 directly relates changes in the OA saturation vapor pressure to changes in its oxidation state. As such, the objective of "connecting the extent of oxidation and the changes in volatility of these experiments with the 2D-VBS framework" was met satisfactorily. Additional studies will need to be conducted to explore whether different systems show different dependencies between oxidation state and vapor pressure. The method of analysis presented in this manuscript could be used in these further studies. The data presented here are some of the first to directly relate measurements of OA saturation vapor pressure and oxidation state and are as such valuable to the research community. This has been made clearer in the revised manuscript.

(16) *Table 1: I suggest adding final concentrations of toluene and also the concentrations of other aromatics added.*

Gas-phase measurements were only available for three out of the nine experiments; all available data have been added to Table 1 of the revised manuscript.

(17) *Table 2: How was NO2 measured? NOx analyzers measure NO2 + organic nitrates, which can be significant.*

The NO and NO_2 data presented in Table 2 refer to measurements of the (particle-phase) NO^+ and NO_2^+ fragments measured by the HR-AMS. We did not attempt to quantify gas-phase NO_2.

(18) *Table 2: Some additional description of how NO/NO2 was determined would be useful. It is not obvious how this was done using linear regressions.*

Particle-phase NO was plotted versus particle-phase NO_2, and a line was fit through the data to obtain the values presented in Table 2. This has been clarified in the revised manuscript.

(19) *Figure 8. It seems like the nice linear relationship here deserves a little more discussion than "Figure 8 shows a comparison of the modeled vs. the measured MFRs." If it is so un-noteworthy perhaps just leave it out.*

Figure 8 shows that the fits work and is therefore noteworthy, but we nevertheless decided to move it to the supplementary material.

Technical Comments:

(20) *Page 31447, bottom line: I suggest using a term other than "molecular ions", since this can be interpreted as non-fragmented ions formed from reaction products, whereas given their low mass these are probably all ion fragments. Perhaps use "ion masses".*

"Molecular ions" was changed to "ion masses" in the revised manuscript.

References

Canagaratna, M. R., Jimenez, J.-L., Kroll, J. H., Chen, Q., Kessler, S. H., Massoli, P., Hildebrandt Ruiz, L., Fortner, E., Williams, L., Wilson, K., Surratt, J. D., Donahue, N. M., Jayne, J. T. and Worsnop, D. R.: Elemental Ratio Measurements of Organic Compounds using Aerosol Mass Spectrometry: Characterization, Improved Calibration, and Implications, Atmos. Chem. Phys., 15, 253–272, 2015.

Epstein, S. a., Riipinen, I. and Donahue, N. M.: A semiempirical correlation between enthalpy of vaporization and saturation concentration for organic aerosol, Environ. Sci. Technol., 44(2), 743–748, doi:10.1021/es902497z, 2010.

Fry, J. L., Kiendler-Scharr, A., Rollins, A. W., Wooldridge, P. J., Brown, S. S., Fuchs, H., Dube, W., Mensah, A., dal Maso, M., Tillmann, R., Dorn, H. P., Brauers, T. and Cohen, R. C.: Organic nitrate and secondary organic aerosol yield from NO3 oxidation of beta-pinene evaluated using a gas-phase kinetics/aerosol partitioning model, Atmos. Chem. Phys., 9, 1431–1449, 2009.

Kostenidou, E., Pathak, R. K. and Pandis, S. N.: An Algorithm for the Calculation of Secondary Organic Aerosol Density Combining AMS and SMPS Data, Aerosol Sci. Technol., 41, 1002–1010, 2007.

Kuwata, M., Zorn, S. R. and Martin, S. T.: Using elemental ratios to predict the density of organic material composed of carbon, hydrogen, and oxygen, Environ. Sci. Technol., 46(2), 787–794, doi:10.1021/es202525q, 2012.

Saleh, R., Donahue, N. M. and Robinson, A. L.: Time Scales for Gas-Particle Partitioning Equilibration of Secondary Organic Aerosol Formed from Alpha-Pinene Ozonolysis, Environ. Sci. Technol., 47, 5588–5594, doi:10.1021/es400078d, 2013.

Seinfeld, J. H. and Pandis, S. N.: Atmospheric Chemistry and Physics, Second Edi., John Wiley & Sons, Hoboken., 2006.

Surratt, J. D., Murphy, S. M., Kroll, J. H., Ng, N. L., Hildebrandt, L., Sorooshian, A., Szmigielski, R., Vermeylen, R., Maenhaut, W., Claeys, M., Flagan, R. C. and Seinfeld, J. H.: Chemical Composition of Secondary Organic Aerosol Formed from the Photooxidation of Isoprene, J. Phys. Chem. A, 110, 9665–9690, 2006.

Formation and Aging of Secondary Organic Aerosol from ~~Small Aromatic VOCs~~Toluene: Changes in Chemical Composition, ~~Mass Yield,~~ Volatility and Hygroscopicity

L. Hildebrandt Ruiz[1,2], A. L. Paciga[2*], K. Cerully[3#], A. Nenes[3], N. M. Donahue[2], S. N. Pandis[2,4]

[1] {The University of Texas at Austin, Austin, Texas, USA}

[2] {Carnegie Mellon University, Pittsburgh, Pennsylvania, USA}

[3] {Georgia Institute of Technology, Atlanta, Georgia, USA}

[4] {University of Patras, Patras, Greece}

[*] Now at Phillips66®, Bartlesville, OK

[#] Now at TSI, Inc., Shoreview, MN

Correspondence to: Lea Hildebrandt Ruiz (lhr@che.utexas.edu)

Abstract

Secondary organic aerosol (SOA) is transformed after its initial formation, but this chemical aging of SOA is poorly understood. Experiments were conducted in the Carnegie Mellon environmental chamber to form ~~and transform~~secondary organic aerosol (~~-~~SOA) from the photo-oxidation of toluene and other small aromatic volatile organic compounds (VOCs) in the presence of NO_x under different oxidizing conditions.~~-~~ The effects of ~~chemical aging~~oxidizing condition on organic aerosol (OA) composition, mass yield, volatility and hygroscopicity were explored. Higher exposure to the hydroxyl radical resulted in different OA composition, average carbon oxidation state (OS_c) and mass yield. The OA oxidation state generally increased during photo-oxidation, and the final OA OS_c ranged from -0.29 to 0.~~45~~ 16 in ~~-~~the performed experiments. The volatility of OA formed in these different experiments varied by as much as a factor of 30, demonstrating that the OA formed under different oxidizing conditions can have significantly different saturation concentration. There was no clear correlation between hygroscopicity and oxidation state for this relatively hygroscopic SOA.

1 Introduction

Secondary organic aerosol (SOA) is produced when gas-phase precursors are oxidized, forming lower volatility products that partition to the condensed phase. As SOA is estimated to account for approximately 70% of total aerosol organic carbon mass (Hallquist et al., 2009), the influence of SOA on aerosol composition and related properties is important and complex (Donahue et al., 2009; Kanakidou et al., 2005; Kroll and Seinfeld, 2008). Using measurements in urban, suburban, and remote sites, Zhang et al. (2007) showed that as aerosol ages in the atmosphere it reaches a highly oxidized state and no longer resembles either fresh primary or secondary aerosol.

Although it is clear that oxidation of gas-phase compounds and continued oxidation of particle-phase compounds play an important role in SOA production and transformation, the underlying chemistry and thermodynamics are poorly understood. Without the correct representation of SOA production and evolution mechanisms, modeling attempts often lead to underestimations of ambient mass loadings (Heald et al., 2005; Volkamer et al., 2006). The large uncertainty in SOA concentrations predicted by Chemical Transport Models (CTMs) demonstrates the need for

experimental data on the multi-generation oxidation reactions or "aging" that lead to changes in mass loadings and physicochemical properties of SOA. Several computational studies have highlighted the importance of not only incorporating extended chemical mechanisms but obtaining corresponding relationships between chemical aging and physiochemical properties of the SOA, such as its volatility, in atmospherically relevant systems (Cappa and Wilson, 2012; Shrivastava et al., 2013).

Considering the current state-of-the-science in aerosol analysis techniques, identifying the plethora of SOA components and their individual volatilities is not possible. A unified framework to evaluate complex systems in field or laboratory studies and to track changes in volatility as a function of physicochemical processing is the 2D-Volatility Basis Set (2D-VBS). It uses coordinates of volatility in terms of effective saturation concentration, C^*, and oxidation state of carbon, OS_c (or the oxygen to carbon ratio, O:C) to provide a space suitable for the description of the chemical transformations and phase partitioning of SOA (Donahue et al., 2012). Chemical species are lumped by C^* and OS_c in discretized bins.

The relationship between organic aerosol (OA) hygroscopicity and extent of oxidation, indicated by O:C, has been the focus of a number of laboratory and field studies (Alfarra et al., 2013; Chang et al., 2010; Frosch et al., 2011; Jimenez et al., 2009; Lathem et al., 2013; Massoli et al., 2010). While OA hygroscopicity often increases with O:C, some other studies have found weak or no correlation between the two properties (Alfarra et al., 2013; Frosch et al., 2011; Lathem et al., 2013; Massoli et al., 2010). It has been shown that OS_c is likely a better indicator of aerosol oxidation than O:C as the latter can be affected by non-oxidative processes such as hydration and dehydration while OS_c increases continually with oxidation (Canagaratna et al., 2015; Kroll et al., 2009, 2011); thus, O:C may not be as well correlated with observed hygroscopicity.

The organic aerosol O:C has been proposed to be linked with its volatility in addition to its hygroscopicity (Jimenez et al., 2009), and a few chamber studies have investigated the link among all three properties (Poulain et al., 2010; Tritscher et al., 2011). The conventional view is that the most volatile components should be the least hygroscopic; however, several studies have observed the opposite behavior (Asa-Awuku et al., 2009; Cerully et al., 2014; Meyer et al., 2009; Poulain et al., 2010). Tritscher et al. (2011) found that hygroscopicity and O:C remained constant with decreased volatility for α-pinene SOA during aging by OH radicals.

We investigated the relationship between oxidation, volatility and hygroscopicity of SOA formed from the photo-oxidation of toluene (methylbenzene) and other small aromatic volatile organic compounds (VOCs) under a variety of oxidation conditions. Small aromatics are important anthropogenic SOA precursors (Pandis et al., 1992; Vutukuru et al., 2006), and toluene serves as a model system to study the formation of SOA from these compounds.

A main objective of our work is ~~is~~ to connect the extent of oxidation and the changes in volatility of these experiments ~~with~~ within the 2D-VBS framework.

2 Materials and Methods

2.1 Environmental Chamber Experiments

Organic aerosol was formed from the photo-oxidation of toluene and other small aromatic VOCs in the Carnegie Mellon Center for Atmospheric Particle Studies (CAPS) environmental chamber. The basic sequence of the experiments was to fill the chamber with clean air, inject the VOC and nitrous acid (HONO), and turn on the UV lights to start formation of OH (from the photolysis of HONO), oxidation of the VOC and formation of secondary organic aerosol (SOA). The number of UV lights used, the initial VOC concentrations, and the number of HONO injections was varied between experiments in order to create different oxidizing environments, as summarized in Table 1. The amount of SOA formed, the SOA oxidation state, its volatility and its hygroscopicity were then measured as explained in more detail below.

Nitrous acid was produced immediately before injection by drop-wise addition of 12 ml 0.1 M sodium nitrite solution to 24 ml 0.05 M sulfuric acid solution. Ammonium sulfate ($(NH_4)_2SO_4$, Sigma Aldrich, 99.99%)) seed particles were used in some experiments (Table 1) to provide surface area onto which organics would condense as SOA. In the unseeded experiments, nucleation of the organic vapors was observed. With the exception of Experiment 7 (Table 1), isotopically labeled toluene was used (^{13}C-toluene, Cambridge Isotope Laboratories, 99%) as in a previous study (Hildebrandt et al., 2011). All six ring carbons in the labeled toluene are ^{13}C-substituted, leaving the methyl carbon unsubstituted. In two experiments (Expts. 6 and 8) other small aromatic compounds were injected in addition to toluene as detailed in Table 1 in order to test whether these VOCs behave similarly as toluene. Concentrations of the VOCs were monitored using a proton-transfer reaction mass spectrometer (PTR-MS, Ionicon Analytik GmbH) when available. PTR-MS measurements ~~of toluene~~ were corrected for ion-source intensity and humidity as suggested by de Gouw et al. (2003). The sensitivity of the PTR-MS to the VOCs was measured before each experiment using a calibration gas mixture~~; calculated sensitivities agreed well with VOC concentrations expected based on the volume of liquid VOC injected~~.

Figure 1 ~~presents~~ illustrates the experimental setup. Particle number and volume of the chamber aerosol were measured using a scanning mobility particle sizer (SMPS), comprised of a TSI model 3080 classifier and a TSI model 3772 condensation particle counter (CPC). Particle mass and

chemical composition was measured using a high-resolution time-of-flight aerosol mass spectrometer (AMS) from Aerodyne, Inc. (DeCarlo et al., 2006). The AMS has two ion optical modes named by the shape of the ion flight paths: a single-reflection mode (V-mode) with a shorter flight path and hence higher sensitivity but lower resolution, and a double-reflection mode (W-mode) with longer flight path and hence higher resolution but lower sensitivity. In this study the AMS was operated according to the common protocol with the vaporizer temperature at 600°C, alternating between V and W modes to collect mass spectra, and collecting particle time-of-flight (pToF) measurements in V-mode.

Air from the chamber was split into two separate streams for analysis of OA concentrations and properties. In the first stream, OA volatility was probed using a thermodenuder (TD) system, similar to the system used in Lee et al. (2010). Aerosol was passed alternately through the TD, heated to a predefined temperature, or a bypass line and then to the SMPS and the AMS for measurements of the particle size distributions and chemical composition. Properties of thermally-treated OA were determined by comparing the residual aerosol after heating in the TD to the aerosol which was passed through the bypass line. The standard operating sample flowrate for the TD was 1 liter per minute (LPM), corresponding to a centerline residence time of ~15 s. In the TD followed by the AMS, the flow rate was also sometimes set to 0.6 LPM, corresponding to a centerline residence time of ~25 s, to evaluate the effects of a longer residence time on OA evaporation, though these data were not used for thermally-denuded CCN comparisons.

In the second stream, aerosol was again passed alternately through the TD or bypass line, then size-selected (approximately 100 to 140 nm) using a differential mobility analyzer (DMA, TSI model 3080) operated with a sheath to aerosol ratio of 10:1. Aerosol flow was then split to a CPC (TSI model 3010) and a cloud condensation nuclei counter (CCNc, Droplet Measurement Technologies). The CCNc was operated in Scanning Flow CCN Analysis (SFCA) mode (Moore et al., 2010), allowing for fast measurements of CCN by scanning the flow rate through the CCNc column, which measured the OA hygroscopicity. The thermodenuder positioned before the CCNc operated under the same temperature conditions as the AMS-TD and had a sample flowrate of 1 LPM, which allows for analysis of volatility and hygroscopicity of the complete OA and the thermally denuded OA. Dilution air of 1.1 LPM was introduced after the DMA before splitting to the CCNc and CPC. Flow to the CCNc was held constant at 1.1 LPM using a laminar flow element,

while flow in the CCNc was linearly ramped between 0.1 and 0.9 L min^{-1} over 60 s. The top to bottom column temperature difference was 6°C for all experiments.

2.2 AMS Data Analysis

The AMS data were processed in Igor Pro 6.12 (Wavemetrics, Inc.) using the standard AMS data analysis toolkits "Squirrel" version 1.51C for unit mass resolution (UMR) analysis and "Pika" version 1.10C for high resolution (HR) analysis. HR analysis was performed using the W-mode data since highest resolution is preferred to distinguish between isotopically labeled and unlabeled ions. The lists of ions integrated in the HR analysis is similar to the list used previously (Hildebrandt et al., 2011). ~~Molecular ions~~Ion masses were fitted up to an *m/z* ratio of 105; above this the signal was too noisy and/or the mass spectra were too crowded for reliable identification of ion atomic composition. According to the UMR analysis more than 95% of the organic signal was below *m/z* 105, and the total organic mass was corrected based on this fraction calculated for each experiment (Table S1). ~~The natural abundance of ^{13}C (1.112%) was accounted for by constraining the mass attributed to fragments containing one ^{13}C based on the concentration of the parent ^{12}C fragments, only attributing any excess signal to ^{13}C toluene SOA. Ions with two or more ^{13}C were not isotopically constrained since their natural abundance is very low and does not significantly affect results.~~

2.2.1 Modification of Standard Fragmentation Table

Several adjustments were made to the standard fragmentation table (Allan et al., 2004) for the analysis of HR and UMR data as explained in detail in the supplementary~~l~~ material; only the most important adjustments are summarized here. First, the fragmentation table was adjusted to account for hydrogen ~~H~~ atoms (*m/z* = 1) formed in the fragmentation of H_2O (Canagaratna et al., ~~2014~~2015). Second, the amount of H_2O^+ attributed to organics was chosen so that the mass of water does not correlate with the mass of organics ($R < 0.01$) as expected for these low relative humidity experiments. The ratios of organic H_2O^+ to ($^{13}CO_2^+ + CO_2^+$) are provided in Table 2 and ranged from 0.3 to 2.4, higher than the ratio of 0.225 in the default fragmentation table but consistent with recent calibration experiments (Canagaratna et al., 2015). Third~~, since no inorganic~~

~~nitrate is added to or expected to be formed in these experiments~~, ions assigned to the nitrate family in the HR analysis (NO^+, NO_2^+) ~~are presumed to be due to organic nitrates and~~ were added to the total organic aerosol mass in the HR batch table because they appear to be due to organic nitrates:~~.~~ The ratio of NO^+ to NO_2^+ measured in these experiments (Table 2) is around 8, much higher than the ratio of 2.4 measured in calibration experiments using ammonium nitrate. Furthermore, no inorganic nitrate was~~is~~ added in these experiments. Nitric acid is expected to form in the gas phase but does not appear to partition appreciably to the particle phase, consistent with its high vapor pressure (Fry et al., 2009). Nitrate fragments were not included in the calculation of O:C and H:C since elemental analysis examines the oxidation state of the carbon atoms.

2.2.2

Quantification of Organic Aerosol Production

Data were corrected for changes in the instrument air beam (AB) over the course of an experiment. The ionization efficiency (IE) for each experiment was adjusted based on the ratio of the AB during the experiment to the AB during the ionization efficiency calibration conducted before this set of experiments was started (calibration IE/AB = 4.65×10^{-13}). Additional details on quantification of AMS data are provided in the supplementary material.~~ Total aerosol concentrations were calculated in the following way to exploit the higher sensitivity (and accuracy) in V-mode and the higher resolution in W-mode. First, UMR fragmentation and batch tables were used to obtain bulk concentration data for sulfate in V and W mode. The V/W ratio was then computed for sulfate, obtaining a measure of the difference in total concentrations measured in these two modes. Second, HR analysis and the HR fragmentation and batch tables were used to obtain organic and sulfate concentrations in W-mode. The W-mode HR data were then multiplied by the (V/W) ratio (from UMR analysis) to obtain the most quantitative estimate of the amount of organic and sulfate mass detected by the AMS. Because all sulfate in these experiments is from the ammonium sulfate seed particles, sulfate mass was multiplied by 1.375 to obtain ammonium sulfate mass. Using the V/W ratio as a correction factor indirectly applies an AB correction in W-mode. When sulfate data were not available, nitrate concentrations in V and W mode were used instead to compute the V/W ratio. The AB and V/W ratio used to correct the data in each experiment are shown in Table S1.~~

2.2.3 Determination of collection efficiency

A further issue with all AMS analysis is that the AMS does not detect all sampled particles, primarily due to particle bounce at the vaporizer. The AMS collection efficiency (CE) for these data was estimated by matching AMS mass distributions and SMPS volume distributions using the OA density (ρ_{org}) and AMS CE as fitting parameters, with the algorithm developed by Kostenidou et al. (Kostenidou et al., 2007) . Particle time of flight (pToF) distributions of organics and sulfate (SO_4^{2-}) from V-mode were used but scaled by the adjusted HR aerosol masses (from MS mode) obtained as described above. The pToF distributions were smoothed before fitting using a 19-point, 2nd order Savitzky-Golay smoothing.

The data from each experiment were split according to whether the OA had been passed through the bypass or the TD to observe whether the denuded OA had a different CE and/or density compared to the total OA. The data from Expt. 9 were further split into a total of 16 periods to explore variation in CE and OA density over the course of an experiment (e.g. with increasing OH exposure of the OA or different denuder temperatures). As can be seen in Fig S1, the CE and OA density did not change significantly over the course of an experiment. There is also very little difference in CE between the OA passed through the bypass or the thermodenuder (Table S1, all experiments). As observed earlier (Lee et al., 2010) the algorithm for estimating AMS CE and OA density is much less sensitive to the OA density than to the AMS CE, and the estimated CE essentially remains the same after fixing the OA density at 1.5 g cm^{-3} (Fig S1). The values of CE are used to correct OA concentrations for the calculation of OA mass yield and mass fraction remaining. Values of OA density are used to convert aerodynamic to mobility diameter for CCN analysis.

2.2.4 Quantifying Organic Aerosol Production

The amount of organic aerosol formed was quantified as the fractional aerosol mass yield (mass of OA formed divided by mass of toluene reacted). The mass of OA formed needs to bewas corrected for the depositional loss of particles onto the chamber walls, and for the condensational loss of organic vapors to wall-deposited particles. The assumption wais made that condensation of organic vapors is not slowed by mass-transfer resistances, and that the wall-deposited particles are in equilibrium with the organic vapors in suspension. Therefore, the total (corrected) concentration of OA can be calculated by multiplying the OA/seed ratio by the initial seed concentration, as

discussed in more detail in Hildebrandt et al. (2009)~~a previous publication (Hildebrandt et al., 2009)~~. This correction does not account for condensation of organic vapors onto the "clean" Teflon ~~®~~ walls. While these losses have been shown to occur (e.g. Matsunaga and Ziemann, 2010), quantification of their magnitude ~~of these losses~~ is an area of active research and remains ~~quite~~ challenging. ~~, and there is no consensus on how to correct for them.~~

In all of the experiments described here, the condensation sink after particle formation was approximately 1 ~~/~~min^{-1}, while the initial condensation sink to ammonium sulfate seeds in seeded experiments ranged between 0.6 and 1 ~~/~~min^{-1}. The timescale for sulfuric acid vapor wall loss in the Carnegie Mellon chamber is approximately 0.1 ~~/~~min^{-1}, as determined by chemical ionization mass spectrometer measurement of sulfuric acid loss (V. Hofbauer, personal communication). Thus, in all of the seeded experiments, condensing vapors encountered the seeds approximately 10 times before encountering the walls, while in nucleation experiments the suspended aerosol population quickly grew to a size where this was also true. Thus, while wall losses of semi-volatile vapors are a source of uncertainty, we have attempted to ensure that vapor-particle interactions at least dominate over vapor-wall interactions. It is therefore reasonable to expect that observed differences between experiments are not driven by interactions with the walls but instead by chemical processing of the organic aerosol.

2.3 Analysis of Organic Aerosol Volatility

2.3.1 Data Preparation

Volatility data were collected for each experiment after the SOA had formed. During some experiments, measurements were also made during the irradiation period (with the UV lights on) to examine the volatility changes during photo-oxidation. TD data are analyzed in terms of Volume Fraction Remaining (VFR) or Mass Fraction Remaining (MFR). Using the total organic mass concentration from the AMS, the MFR was calculated by dividing the mass concentration of the denuded OA by the mass concentration of the OA that had passed through the bypass. These data are presented in the form of a thermogram, which shows the MFR as a function of temperature in the TD.

Particle concentrations decline in the smog chamber after SOA formation chemistry ceases due to losses to the chamber walls. This can lead to biases in the estimated MFR when bypass concentrations before or after the TD sampling period are used. A more accurate MFR was obtained by interpolation of the bypass OA concentrations corresponding to the TD sampling times. Each experiment was analyzed individually for a best fit, usually resulting in an exponential decay function. Graphs of the interpolated bypass data are shown in Fig S2.

Particle losses in the TD were also taken into account. These losses occur due to diffusion (primarily of small particles), sedimentation (primarily of large particles), and thermophoresis; the losses are therefore a function of sample flow rate, temperature, and particle size (Burtscher et al., 2001). To estimate the losses within the TD setup, size dependent loss functions were developed using NaCl particles under various TD temperatures and sample flow rates (Lee and Pandis, 2010). The number losses for each TD temperature – residence time combination are calculated by determining the losses over the size distribution measured by the SMPS. The number losses for each size bin are then converted to a volume-based correction using the particle diameter of each bin. This correction factor is applied to the calculated MFR values. The organic MFR was calculated from AMS bypass and thermodenuder mass concentrations averaged over 6-9 minutes for a given TD temperature and residence time. It is assumed that there are no significant changes to composition and volatility over these averaging periods.

2.3.2 Evaporation model

Due to the non-equilibrium conditions in the TD, a dynamic mass transfer model developed by Riipinen et al. (2010) was used to estimate the relative volatility of the OA formed in the experiments outlined in Table 1. Briefly, aerosol evaporation is simulated using experimental inputs including TD temperature, residence time, particle mode diameter, mass concentration, and OA density. This method utilizes the volatility basis set approach (Donahue et al., 2006) to account for the component complexity in the SOA formed. Assuming the particles are in equilibrium with the vapor phase as they enter the TD, the effective saturation concentration is estimated from a least-squares fit to the experimental thermograms. An important caveat to this approach is that physical properties including mass accommodation coefficient and enthalpy of vaporization, which are usually unknown, can substantially affect the volatility estimated (Lee et al., 2010) . The primary goal of these experiments was to observe changes in OA volatility with different levels of

oxidation. Thus, relative volatility changes were calculated as described below, thus reducing uncertainties arising from the choice of accommodation coefficient and enthalpy of vaporization.

The volatility of SOA formed in each experiment was determined assuming a fixed volatility distribution shape using four saturation concentrations, 1, 10, 100, and 1000 μg m^{-3}. During the analysis the saturation concentrations are multiplied by a shifting factor, *s*. This practically shifts the volatility distribution to lower or higher values assuming that the shape of the distribution does not change. ~~The~~ Differences in shifting factors can then be interpreted as differences in ~~volatility~~ the saturation vapor pressure of the OA formed in these~~different~~ experiments: for example, OA with shifting factor 10 is ten~~10~~ times more volatile than the OA with shifting factor 1.~~a shifting factor of 10 corresponds to an increase in volatility of one order of magnitude~~. The volatility distribution used is ~~based on~~ the fresh toluene SOA distribution estimated by Hildebrandt et al. (2009) for their high NO_x experiments: 0.025 for C^* = 1, 0.51 for C^* = 10, 0.38 for C^* = 100, and 0.085 for C^* = 1000 μg m^{-3}. The shifting factor is estimated for each of the experiments presented here by using the mass transfer model and least squares fitting to the MFRs. In the last step relative shifting factors are calculated by normalizing them by the shifting factor of the OA formed in Expt. 7, in which SOA had the lowest OS_c. In this way, the relative volatility reduction (1/*s*) for each experiment is estimated while accounting for the experiment specifics including residence time, TD temperature, mass concentration, and particle size. Fixed values are used for the enthalpy of vaporization (80 kJ mol^{-1}) and the mass accommodation coefficient (1.0). The sensitivity of results to these choices ~~will be~~is~~are~~ discussed in Section 3.2.

2.4 Analysis of CCN Activity

2.4.1 CCNc calibration

The CCNc instrument calibration is used to determine the relationship between instantaneous instrument flow rate and supersaturation as described in Moore et al. (2010). Ammonium sulfate solution is atomized, dried using a silica gel diffusion dryer, charge-neutralized using Po-210, and classified by a DMA. The flow is then introduced into both a CPC and a CCNc. The activation ratio, or the ratio of CCN to total particles, is then plotted against the instantaneous flow rate to yield data that are fit to a sigmoidal activation ratio function. The critical flow rate, Q^*, is determined, corresponding to where half of the total particles are activated and to a level of

supersaturation, s^*, equal to the critical supersaturation of the classified aerosol (Section 2.4.2). The Q^* and s^* are determined for a range of aerosol sizes, yielding, for the flow rate range (0.1-0.9 L min^{-1}) and temperature gradient (ΔT=6°C) in the CCNc column, supersaturations ranging from approximately 0.1~~θ~~ to 0.5~~θ~~%.

2.4.2 Calculating aerosol hygroscopicity of size-selected aerosol

Using the method outlined in Section 2.4.1, s^* was determined for each flow rate upscan and downscan. All CCNc data subject to poor counting statistics (where the maximum CCN concentrations were lower than approximately 15 to 20 counts cm^{-3}) were excluded from analysis (Moore et al., 2010). The characteristic hygroscopicity parameter, κ (Petters and Kreidenweis, 2007), of the monodisperse CCN is then determined by

$$\kappa = \frac{4A^3}{27 d_p^3 s^{*2}} \quad (1)$$

where $A=(4M_w\sigma_w)/(RT\rho_w)$; M_w, σ_w, and ρ_w are the molar mass, surface tension, and density of water, respectively. R is the universal gas constant, T is CCNc mid-column temperature, and d_p is the dry particle diameter selected by the DMA prior to the CCNc.

3 Results and Discussion

3.1 Organic aerosol concentration, composition and mass yield

Figure 2 shows the time series of OA concentrations and oxidation state for an unseeded experiment (2, top panel) and a seeded experiment (9, bottom panel). The time series of toluene concentrations are also shown for Expt. 9; these data were not available for Expt. 2. There were two photo-oxidation periods ("lights on") during each experiment, and HONO was injected every time before lights were turned on. During experiment 2, the OA was alternatively passed through the bypass and the TD throughout the experiment (only the bypass data are shown in Fig 2). The TD was held at the same temperature during the photo-oxidation periods to observe changes in volatility during this period, and the temperature in the TD was varied during the dark period to obtain a thermogram. During experiment 9, the OA was passed only through the bypass during

photo-oxidation, and it was alternated between bypass and TD (at different temperatures) during the dark period. The OA concentrations increased during the oxidation periods (lights on) as toluene ~~(not shown)~~ was oxidized to form SOA. Toluene concentrations decreased by approximately 50% during the first photo-oxidation period in Expt. 9 and decreased an additional 20% during the second photo-oxidation period. Thus, gas-phase toluene is always present in the system and fresh toluene SOA is expected to form at the same time as the previously formed toluene SOA is aged photo-chemically.

~~The behavior of oxidation state was different for these two experiments~~A moderate increase in the OA oxidation state was observed during the "lights on" period in both experiments. ~~In Expt. 2 the oxidation state was initially very high (~3), consistent with very highly oxidized, low-volatility organic compounds nucleating to form new particles. After the initial formation of particles t~~Two competing effects can influence the OA oxidation state: First, according to partitioning theory, species of increasingly higher volatility will partition to the particle phase as the OA loading in the system increases. If oxidation state is anti-correlated with volatility this effect would decrease oxidation state when OA concentration increases. Second, the existing OA can be oxidized further (aged), increasing the OA oxidation state as long as the molecules composing the OA do not fragment. T~~he oxidation state of the OA formed in Expt. 2 first decreased and then increased during both irradiation periods, suggesting that first the partitioning effect and then the aging effect dominated. In Expt. 9 and~~he OA oxidation state of the OA formed ~~all other experiments conducted the oxidation state of the OA formed~~ increased ~~sed over the course of the experiments~~during the ~~first few~~for several h–ours in the experiments shown in Figure 2 and all other experiments conducted as part of this work, suggesting that the aging effect ~~always~~ dominated. ~~The OA formed in Expt. 2 had a much higher oxidation state than the OA formed in the other experiments (Table 2); hence it appears that the aging effect dominates in these experiments unless the OA oxidation state is already very high.~~

In an attempt to produce highly oxidized OA, photo-oxidation of the OA was continued for over 24 hours during experiments 3 and 5. Figure 3 shows the time series of oxidation state and elemental ratios (O:C and H:C) for ~~experiment~~ Expt. 3. As before, HONO was injected before every irradiation period. The OA oxidation state increased during the first few hours of irradiation but significantly ~~A significant~~ decreased ~~in oxidation state and O:C was observed during the~~after longer irradiation ~~long irradiation period~~. Plausible explanations for this decrease in oxidation state

(which was also observed after long irradiation in experiment 5) include the condensation of less oxidized vapors, ~~that~~ photolysis of OA components ~~are photolyzed, or that they~~ and their fragmentation after continued oxidation with OH~~. . In the last two cases the f~~Fragmented products may have a high oxidation state but high volatility (due to their smaller size) and evaporate from the OA, decreasing the OA average oxidation state. Photolysis of organic compounds is expected to occur throughout the experiment (e.g. Surratt et al., 2006), but as long as OH reactions dominate the oxidation state of the bulk OA increases. Future experiments should aim to isolate OH from photolysis reactions by, for example, using a dark OH source. This would help to constrain these effects and eventually represent them in chemical transport models.

Table 2 provides a summary of the OA composition for all experiments investigated here. The observed oxidation state of the OA formed ranged from -0.29 to 0.~~45~~16. At least 10% of the OA mass was due to the sum of NO^+ and NO_2^+ ions. The observed ratio of NO^+ to NO_2^+ (Table 2) was between 7.0 and 8.6, ~~much higher than~~much higher than the ratio of 2.4 measured in calibration experiments using ammonium nitrate~~ typically observed ratios for NH_4NO_3 (Farmer et al., 2010)~~, suggesting that the NO^+ and NO_2^+ ions originate from organic nitrogen (ON) compounds. Estimating that the ON compounds have an average molecular weight of about 200 g mol^{-1}, approximately half of the OA is due to ON. Thus, organic nitrogen compounds are a major constituent in the OA formed in these high-NO_x photo-oxidation experiments.

In experiments 6 and 8, other small aromatic VOCs were injected in addition to toluene. The OA formed in these experiments did not stand out in terms of its composition, volatility (Section 3.3) or hygroscopicity (Section 3.4). This suggests that other small aromatic VOCs behave similarly as toluene and that toluene can be used as a model system to study small aromatic VOCs.

~~The HR data can shed light on the different roles of the methyl carbon atom (methyl-C) and the aromatic-Cs in the photo-oxidation reactions. (Recall that the aromatic-Cs on the ^{13}C-toluene are isotopically substituted but the methyl-C is not.) Table 2 lists the average ratio CO_2:$^{13}CO_2$ for all experiments. In experiments 1-5 and experiment 9, only ^{13}C-toluene SOA was present in the system, so $^{12}CO_2$ originates from the methyl-C on ^{13}C-toluene. If the methyl-C behaved as the aromatic-Cs, the expected ratio of CO_2:$^{13}CO_2$ would be 1/6. However, CO_2:$^{13}CO_2$ is about threefold lower than this. The CO_2^+ fragment observed in AMS data is thought to originate primarily from organic acid functional groups; hence, this observation suggests that the methyl-C~~

~~is about three times less likely than the aromatic Cs to form organic acids in these photo-oxidation reactions.~~

3.2 High and low oxidation experiments – a case study

This section compares two seeded experiments (number 7 and 9, Table 1) and two unseeded experiments (number 2 and 4). The aim in the design of these experiments was to create ~~very~~ different photochemical conditions. Therefore, ~~less~~ fewer HONO injections were performed, ~~and~~ more toluene was injected, fewer lights were used (resulting in lower UV intensity), and the irradiation period was shorter in Expt. 7 compared to Expt. 9 (10 minutes and 3 hours, respectively). The decay of toluene, monitored by the PTR-MS, was used to estimate the OH exposure of the OA during irradiation. T~~t~~otal OH exposure during Expt. 7 was 7-8 times lower than during Expt. 9. Figure 4 shows the OA mass yields for experiments 7 and 9 as a function of the corrected OA concentration in the system; only the first irradiation period was used for Expt. 9 as uncertainties due to wall losses increase over the course of an experiment.~~.~~ The OA yields are higher for Expt. 9, which exhibited higher OH exposure. Considering only the first irradiation period, OH exposure in Expt. 9 was five times higher than in Expt. 9. The OA formed in Expt. 9 also exhibited significantly higher oxidation state (~0, Table 2) than the OA formed in Expt. 7 (~-0.3), and its volatility was approximately a factor of seven lower than the volatility of the OA formed in Expt. 7 (Table 2). ~~The SOA loading was approximately twice as high in Expt. 7 compared to Expt. 9.~~

~~Recent~~Previous work has suggested that higher OH exposures help to reduce wall losses (Kroll et al., 2007); therefore, ~~-~~different oxidizing conditions could result in different wall-loss rates of semi volatile vapors. As mentioned in section 2.2.2 above the changes observed in these experiments seem to be driven by chemical processes, not by the interactions with chamber walls. Thus,~~Higher~~ the higher oxidation state and lower volatility observed ~~OH exposure~~ during Expt. 9 ~~resulted in different OA composition, reflected in a higher oxidation state and lower volatility.~~ were likely a result of higher OH exposure.

The OA mass yields shown in Fig 4 are lower than high NO_x OA mass yield measured in our previous study (Hildebrandt et al., 2009), likely due to different initial and oxidizing conditions. In the previous study the source of OH and NO_x was HOOH and NO, and all NO converted to

NO_2 within a few minutes of the start of photo-oxidation. In the present study the source of OH and NO_x was HONO, and both NO and NO_2 were present throughout the experiments. Gas-phase chemistry is primarily affected by the level of NO, not total NO_x, and lower OA mass yields are expected under high NO, high NO_x conditions (present study) compared to high NOx low NO conditions (Hildebrandt et al., 2009).

Differences in the OA composition are also apparent when comparing the total OA to the denuded OA from these two experiments. Figure 5 (right panel) shows the difference in oxidation state of the denuded and the total OA at the different TD temperatures for Expt. 7 and 9. For the less oxidized, more volatile OA formed in Expt. 7, the oxidation state of the denuded OA is higher than the oxidation state of the total OA, as expected when volatility correlates with oxidation state. The difference is larger at the higher TD temperatures when a larger fraction of the total OA has evaporated. However, for the more oxidized, less volatile OA formed in Expt. 9, the denuded OA has essentially the same oxidation state as the total OA at all TD temperatures. This is consistent with the OA being composed of molecules that have a similar oxidation state but different chain length, resulting in different volatilities. A similar observation was made when sampling highly oxygenated OA during ambient measurements in Finokalia, Greece, where the fraction of OA due to fragments of *m/z* 44 was not significantly different for denuded and total OA (Hildebrandt et al., 2010).

A similar comparison can be made for two non-seeded experiments (number 2 and 4), which resulted in OA of different oxidation state and volatility (Table 2). ~~The experimental conditions were designed to be similar for these two experiments (Table 1); however, the HONO source is difficult to control, and it is likely that higher OH concentrations as well as lower OA concentrations in Expt. 2 resulted in the more oxidized, less volatile OA.~~ Data from the PTR-MS were not available for this experiment, hence, OH exposure could not be estimated and OA mass yields could not be calculated, but it is likely that higher OH concentrations as well as lower OA concentrations in Expt. 2 resulted in the more oxidized, less volatile OA. The OA formed in Expt. 4 had similar oxidation state as the OA formed in Expt. 9 mentioned above (~ 0). The OA formed in Expt. 2 had the highest oxidation state of all OA analyzed here (~ 0.~~45~~16), and its volatility was about a factor of seven lower than the volatility of the OA formed in Expt. 4. The left panel of Fig 5 shows the difference in oxidation state (denuded vs. total) as a function of TD temperature for Expts. 2 and 4. The OA formed in Expt. 4 exhibits similar behavior as the OA formed in Expt. 9,

with very little difference between the oxidation state of denuded and total OA. The OA in Expt. 2 shows a higher oxidation state for denuded OA than for non-denuded OA. Thus, it appears that for OA of lower and higher bulk oxidation state, the oxidation state anti-correlates with volatility, shown here as a higher oxidation state of the denuded OA. For OA of intermediate oxidation state (around zero), the volatility of the OA does not correlate significantly with bulk oxidation state. ~~The bulk oxidation state of OA formed in one experiment does not always correlate with its volatility.~~ The ~~OA~~ volatility and oxidation state of OA formed in all ~~of all~~ experiments is analyzed further below.

3.3 Volatility

Figure 6 shows mass concentration time series measured during Experiment 7 including both the bypass and TD measurements. This experiment produced the least oxidized and most volatile SOA and serves as the baseline for ~~our~~ comparison~~analysis~~ of OA volatility in the other experiments. HONO was injected into the chamber and, at t = 0, the UV lights ~~(30% of them)~~ in the chamber (30% of them) were turned on. The hydroxyl radical formed during the HONO photolysis began to react with toluene and the organic mass concentration increased due to the formation of SOA. The lights remained on for approximately 15 minutes and at that point the HONO photolysis was stopped by turning off the UV lights. The AMS then alternated between the bypass line and thermodenuder (operating at different temperatures and residence times) to obtain the thermogram shown in Fig 7. Half of the organic aerosol mass evaporated at 70 ~~-~~°C (T_{50} temperature). For this and all other experiments, the MFR was nearly the same after 15 and 25 seconds residence time in the thermodenuder.

The 15 and 25 s residence time datasets were independently modeled, resulting in two estimates of volatility reduction for each experiment. These were quite similar (Table 2) for all cases suggesting that these measurements are consistent with the choice of a unity accommodation coefficient. The estimated relative volatility reductions relative to Experiment 7 for all experiments are presented in Table 2, and the experiment-specific model inputs (OA loading, particle mode diameter, and OA density) are presented in Table ~~S3~~S2. Volatility was lower in other experiments by as much as a factor of 30, demonstrating that the OA formed under different oxidation conditions can have significantly different ~~vapor pressure~~vapor pressure ~~under different oxidation~~

~~conditions~~. ~~Figure 8 shows a~~A comparison of the modeled versus the measured MFRs is shown in Figure S3.

Sensitivity runs were performed in order to~~To~~ examine the effects of the accommodation coefficient and enthalpy of vaporization parameters~~, sensitivity runs were performed~~. In summary, the analysis revealed that changing the mass accommodation coefficients between 0.01, 0.1 and 1 for Expts. 7 and 9, which exhibited quite different experimental conditions, changes neither the relative volatility reduction nor the goodness of fit (represented by the sum of squared residuals, SSR) by more than 15%. In addition, better least squares fits are obtained for enthalpy of vaporization of 80 kJ mol^{-1} (average SSR for all nine experiments, $SSR_{avg} = 0.04$) than for enthalpy of vaporizations of 20 kJ mol^{-1} or 120 kJ mol^{-1} ($SSR_{avg} = 0.11$ and 0.09, respectively). Changing the enthalpy of vaporization does not change the trends in volatility reduction between experiments. ~~Detailed~~ More detailed results of the sensitivity study are presented in the supplementary~~l~~ material.

3.3.1 Dependence of Volatility on Oxidation State

~~The change~~Differences in volatility of the toluene SOA in these experiments can be compared to its carbon oxidation state (Fig. ~~9~~8). The change in volatility is expressed as the logarithm of the volatility reduction. This is consistent with the assumption of a constant volatility distribution shape shifting. Each data point represents a single experiment in terms of volatility reduction or the change in log C^* and the corresponding ~~carbon oxidation state~~OS_c. In general, the more oxidized organic aerosol is less volatile. This is consistent with functionalization reactions decreasing the volatility of the OA as it is oxidized. Using a least squares fit, a straight line is fit to the dataset giving a relation of $(OS_c) = 0.4~~67~~284 (\Delta\log_{10} C^*) - 0.3~~24~~245$. This suggests that an increase of the oxidation state by approximately 0.~~5~~3 units corresponds to a reduction of the average volatility by an order of magnitude for the toluene SOA system examined here. However, as ~~we have noted above~~ discussed in section 3.2, the volatility of individual species composing the OA is not always correlated to ~~its~~ their oxidation state.

3.4 Hygroscopicity

CCNc-derived organic hygroscopicity, κ_{org}, expressed as the average hygroscopicity of all measured sizes, versus the bulk O:C ratio and OS_c is shown in Fig. ~~10~~ 9 for each experiment where CCNc data were available. Throughout all experiments, κ_{org} ranges from 0.10 to 0.25 while bulk O:C ranges from approximately 0.85 to 1.05. For each experiment, after the initial period of photo-oxidation, κ_{org} remains fairly constant, as does O:C. There is no clear correlation between κ_{org} and O:C (Fig ~~10~~ 9 top, left) or between κ_{org} and OS_c (Fig. ~~10~~ 9 top, right) across all experimental conditions. ~~Thus~~ This is counter to the conventional view that oxidative aging of aerosol generally increases its hygroscopicity ~~(~~(Jimenez et al., 2009).

When investigating κ_{org} for Expts. 4 and 6 where both non-denuded and thermally-denuded measurements were collected, it appears that thermally-denuded aerosol (combined measurements from 60, 80, and 100°C) may show a slight decrease in κ_{org} with increased O:C (and OS_c) (Fig. ~~10~~ 9 bottom). While the change in κ_{org} as well as O:C and OS_c cannot be concluded with confidence due to the relatively large variation in κ_{org}, it is possible that this relationship between hygroscopicity and oxidation suggests that there may be another process, aside from bulk oxidation changes, causing changes in the measured hygroscopicity. Sareen et al. (2013) showed that gas-phase compounds such as methylglyoxal can act as surfactants, which depress surface tension and enhance CCN-activity (and hygroscopicity). As methylglyoxal as well as other gas-phase surface-active compounds such as benzaldehyde and glyoxal are known products of toluene oxidation by OH (Baltaretu et al., 2009), it is likely that gas-phase surfactants are present ~~here~~in these experiments. If surfactant films are present on the non-denuded aerosol, enhancing their hygroscopicity, then desorption of the surfactants later upon heating may increase surface tension and depress apparent hygroscopicity. A monolayer of surfactant adsorbed from the gas phase would induce a negligible impact on bulk O:C or OS_c. Thus, the volatility of OA would not necessarily correlate with its oxidation state if surfactants are present.~~, thus it is expected, as seen here, that the least volatile aerosol is the most oxidized.~~

Another potential explanation for the lack of a clear correlation between κ_{org} and OS_c ~~would be~~is that the OA composition is dominated by compounds with similar OS_c but different ~~chain length~~size ~~-~~(e.g~~i.e~~. oligomers)~~. The size of the molecules~~ , as the size of molecules affects their solubility and therefore their hygroscopicity.

4 Conclusions

Photochemical aging clearly influences anthropogenic SOA, and the general trend toward increased SOA mass and reduced volatility is consistent with progressive oxidation driving organic aerosol toward the highly oxidized, low-volatility endpoint observed around the world. There is a strong relationship between exposure to OH and physicochemical properties for SOA formed from the oxidation of toluene and other small aromatic -VOCs. Organic nitrogen compounds ~~we~~are a major constituent in the SOA formed. ~~Experiments~~ An experiment with higher OH exposure showed higher SOA mass yields, more oxidized SOA, and reduced SOA volatility but only modest differences in hygroscopicity. Volatility varied by a factor of 30 for different OH exposure, and a ten-fold decrease in volatility was associated with a 0.~~5~~ 3 increase in carbon oxidation state. The SOA was relatively hygroscopic for organic material, with $0.1 < \kappa < 0.2$ and if anything a slightly negative relationship between kappa and oxidation state was observed,~~,~~ suggesting a possible role for surfactants or oligomeric compound~~s.~~ s. The relationship between hygroscopicity, oxidation state and volatility may be modulated by gas-phase compounds.~~Organic nitrogen compounds were a major constituent in the SOA formed. Use of isotopically labeled toluene revealed that the methyl carbon atom of toluene is about three times less likely than the aromatic carbon atoms to form organic acids in these photo-oxidation reactions.~~

While individual experiments with different OH exposure ~~revealed~~ showed clear aging effects as different oxidation states and OA volatility, these effects were ~~generally~~ not evident within ~~a single~~every single experiment~~, even with photo-oxidation extending over many hours~~. This ~~dichotomy remains a puzzle, suggesting~~ suggests that a complex interplay exists between gas-phase processes, including oxidation reactions that both functionalize and fragment condensable organic species as well as photolysis of some species. The composition, hygroscopicity and volatility of organic aerosol do not always follow a prescribed relationship, ~~and~~ highlighting the need for ~~additional~~future ~~studies~~ laboratory experiments and ambient measurements ~~are needed~~ which evaluate~~d~~ all of these properties~~ in future laboratory experiments and ambient measurements~~.

~~Photochemical aging clearly influences anthropogenic SOA, and the general trend toward increased SOA mass and reduced volatility is consistent with progressive oxidation driving organic aerosol toward the highly oxidized, low-volatility endpoint observed around the world. However, especially for aromatic compounds, the specific mechanistic steps along this path remain enigmatic.~~

Acknowledgements

This work was supported by the EPA STAR program (grant RD-835405) and the Department of Energy Atmospheric Science Research Program (ASR grant DESC0007075). The high-resolution AMS was purchased with funds from NSF Major Research Instrumentation (CBET0922643) and the Wallace Research Foundation.

References

Alfarra, M. R., Good, N., Wyche, K. P., Hamilton, J. F., Monks, P. S., Lewis, A. C. and McFiggans, G.: Water uptake is independent of the inferred composition of secondary aerosols derived from multiple biogenic VOCs, Atmos. Chem. Phys., 13, 11769–11789, doi:10.5194/acp-13-11769-2013, 2013.

Allan, J. D., Delia, A. E., Coe, H., Bower, K. N., Alfarra, M. R., Jimenez, J. L., Middlebrook, A. M., Drewnick, F., Onasch, T. B., Canagaratna, M. R., Jayne, J. T. and Worsnop, D. R.: A generalised method for the extraction of chemically resolved mass spectra from Aerodyne aerosol mass spectrometer data, J. Aerosol Sci., 35(7), 909–922, doi:10.1016/j.jaerosci.2004.02.007, 2004.

Asa-Awuku, A., Engelhart, G. J., Lee, B. H., Pandis, S. N. and Nenes, A.: Relating CCN activity, volatility, and droplet growth kinetics of beta-caryophyllene secondary organic aerosol, Atmos. Chem. Phys., 9, 795–812, doi:10.5194/acp-9-795-2009, 2009.

Baltaretu, C. O., Lichtman, E. I., Hadler, A. B. and Elrod, M. J.: Primary atmospheric oxidation mechanism for toluene., J. Phys. Chem. A, 113(1), 221–30, doi:10.1021/jp806841t, 2009.

Burtscher, H., Baltensperger, U., Bukowiecki, N., Cohn, P., Huglin, C., Mohr, M., Matter, U., Nyeki, S., Schmatloch, V., Streit, N. and Weingartner, E.: Separation of volatile and non-volatile aerosol fractions by thermodesorption: Instrumental development and applications, J. Aerosol Sci., 32, 427–442, doi:10.1016/S0021-8502(00)00089-6, 2001.

Canagaratna, M. R., Jimenez, J.-L., Kroll, J. H., Chen, Q., Kessler, S. H., Massoli, P., Hildebrandt Ruiz, L., Fortner, E., Williams, L., Wilson, K., Surratt, J. D., Donahue, N. M., Jayne, J. T. and Worsnop, D. R.: Elemental Ratio Measurements of Organic Compounds using Aerosol Mass Spectrometry: Characterization, Improved Calibration, and Implications, Atmos. Chem. Phys., 15, 253–272, doi:10.5194/acp-15-253-2015, 2015.

Cappa, C. D. and Wilson, K. R.: Multi-generation gas-phase oxidation, equilibrium partitioning, and the formation and evolution of secondary organic aerosol, Atmos. Chem. Phys., 12, 9505–9528, doi:10.5194/acp-12-9505-2012, 2012.

Cerully, K. M., Bougiatioti, A., Hite Jr, J. R., Guo, H., Xu, L., Ng, N. L., Weber, R. and Nenes, A.: On the link between hygroscopicity, volatility, and oxidation state of ambient and water-soluble aerosol in the Southeastern United States, Atmos. Chem. Phys. Discuss., 14, 30835–30877, 2014.

Chang, R. Y.-W., Slowik, J. G., Shantz, N. C., Vlasenko, a., Liggio, J., Sjostedt, S. J., Leaitch, W. R. and Abbatt, J. P. D.: The hygroscopicity parameter (κ) of ambient organic aerosol at a field site subject to biogenic and anthropogenic influences: relationship to degree of aerosol oxidation, Atmos. Chem. Phys., 10, 5047–5064, doi:10.5194/acp-10-5047-2010, 2010.

DeCarlo, P. F., Kimmel, J. R., Trimborn, A. M., Northway, M. J., Jayne, J. T., Aiken, A. C., Gonin, M., Fuhrer, K., Horvath, T., Docherty, K. S., Worsnop, D. R. and Jimenez, J. L.: Field-Deployable, High-Resolution, Time-of-Flight Aerosol Mass Spectrometer, Anal. Chem., 78, 8281–8289, 2006.

Donahue, N. M., Kroll, J. H., Pandis, S. N. and Robinson, a. L.: A two-dimensional volatility basis set – Part 2: Diagnostics of organic-aerosol evolution, Atmos. Chem. Phys., 12, 615–634, doi:10.5194/acp-12-615-2012, 2012.

Donahue, N. M., Robinson, A. L. and Pandis, S. N.: Atmospheric organic particulate matter: From smoke to secondary organic aerosol, Atmos. Environ., 43, 94–106, 2009.

Donahue, N. M., Robinson, A. L., Stanier, C. O. and Pandis, S. N.: Coupled Partitioning, Dilution, and Chemical Aging of Semivolatile Organics, Environ. Sci. Technol., 40, 2635–2643, doi:10.1021/es052297c, 2006.

Frosch, M., Bilde, M., DeCarlo, P. F., Juranyi, Z., Tritscher, T., Dommen, J., Donahue, N. M., Gysel, M., Weingartner, E. and Baltensperger, U.: Relating cloud condensation nuclei activity and oxidation level of α-pinene secondary organic aerosols, J. Geophys. Res., 116(D2212), doi:10.1029/2011JD01640, 2011.

Fry, J. L., Kiendler-Scharr, A., Rollins, A. W., Wooldridge, P. J., Brown, S. S., Fuchs, H., Dube, W., Mensah, A., dal Maso, M., Tillmann, R., Dorn, H. P., Brauers, T. and Cohen, R. C.: Organic nitrate and secondary organic aerosol yield from NO3 oxidation of beta-pinene evaluated using a gas-phase kinetics/aerosol partitioning model, Atmos. Chem. Phys., 9, 1431–1449, doi:10.5194/acp-9-1431-2009, 2009.

De Gouw, J. A., Goldan, P. D., Warneke, C., Kuster, W. C., Roberts, J. M., Marchewka, M., Bertman, S. B., Pszenny, A. A. P. and Keene, W. C.: Validation of proton transfer reaction-mass spectrometry (PTR-MS) measurements of gas-phase organic compounds in the atmosphere during the New England Air Quality Study (NEAQS) in 2002, J. Geophys. Res., 108(D21), 4682, doi:10.1029/2003JD003863, 2003.

Hallquist, M., Wenger, J. C., Baltensperger, U., Rudich, Y., Simpson, D., Claeys, M., Dommen, J., Donahue, N. M., George, C., Goldstein, a. H., Hamilton, J. F., Herrmann, H., Hoffmann, T., Iinuma, Y., Jang, M., Jenkin, M., Jimenez, J. L., Kiendler-Scharr, a., Maenhaut, W., McFiggans, G., Mentel, T. F., Monod, a., Prévôt, a. S. H., Seinfeld, J. H., Surratt, J. D., Szmigielski, R. and

Wildt, J.: The formation, properties and impact of secondary organic aerosol: current and emerging issues, Atmos. Chem. Phys., 9, 5155-5236, doi:10.5194/acp-9-5155-2009, 2009.

Heald, C. L., Jacob, D. J., Park, R. J., Russell, L. M., Huebert, B. J., Seinfeld, J. H., Liao, H. and Weber, R. J.: A large organic aerosol source in the free troposphere missing from current models, Geophys. Res. Lett., 32(L18809), doi:10.1029/2005GL023831, 2005.

Hildebrandt, L., Donahue, N. M. and Pandis, S. N.: High formation of secondary organic aerosol from the photo-oxidation of toluene, Atmos. Chem. Phys., 9, 2973–2986, doi:10.5194/acp-9-2973-2009, 2009.

Hildebrandt, L., Henry, K., Kroll, J. H., Pandis, S. N. and Donahue, N. M.: Evaluating the Mixing of Organic Aerosol Components using High-Resolution Aerosol Mass Spectrometry, Environ. Sci. Technol., 45, 6329–6335, doi:10.1021/es200825g, 2011.

Hildebrandt, L., Kostenidou, E., Mihalopoulos, N., Worsnop, D. R., Donahue, N. M. and Pandis, S. N.: Formation of highly oxygenated organic aerosol in the atmosphere: Insights from the Finokalia Aerosol Measurement Experiments, Geophys. Res. Lett., 37 (L23801), doi:10.1029/2010GL045193, 2010.

Jimenez, J. L., Canagaratna, M. R., Donahue, N. M., Prevot, a S. H., Zhang, Q., Kroll, J. H., DeCarlo, P. F., Allan, J. D., Coe, H., Ng, N. L., Aiken, a C., Docherty, K. S., Ulbrich, I. M., Grieshop, a P., Robinson, a L., Duplissy, J., Smith, J. D., Wilson, K. R., Lanz, V. a, Hueglin, C., Sun, Y. L., Tian, J., Laaksonen, a, Raatikainen, T., Rautiainen, J., Vaattovaara, P., Ehn, M., Kulmala, M., Tomlinson, J. M., Collins, D. R., Cubison, M. J., Dunlea, E. J., Huffman, J. a, Onasch, T. B., Alfarra, M. R., Williams, P. I., Bower, K., Kondo, Y., Schneider, J., Drewnick, F., Borrmann, S., Weimer, S., Demerjian, K., Salcedo, D., Cottrell, L., Griffin, R., Takami, a, Miyoshi, T., Hatakeyama, S., Shimono, a, Sun, J. Y., Zhang, Y. M., Dzepina, K., Kimmel, J. R., Sueper, D., Jayne, J. T., Herndon, S. C., Trimborn, a M., Williams, L. R., Wood, E. C., Middlebrook, a M., Kolb, C. E., Baltensperger, U. and Worsnop, D. R.: Evolution of organic aerosols in the atmosphere., Science, 326(5959), 1525–9, doi:10.1126/science.1180353, 2009.

Kanakidou, M., Seinfeld, J. H., Pandis, S. N., Barnes, I., Dentener, F. J., Facchini, M. C., Van Dingenen, R., Ervens, B., Nenes, A., Nielsen, C. J., Swietlicki, E., Putaud, J. P., Balkanski, Y., Fuzzi, S., Horth, J., Moortgat, G. K., Winterhalter, R., Myhre, C. E. L., Tsigaridis, K., Vignati, E., Stephanou, E. G. and Wilson, J.: Organic aerosol and global climate modelling: a review, Atmos. Chem. Phys., 5, 1053–1123, doi:10.5194/acp-5-1053-2005, 2005.

Kostenidou, E., Pathak, R. K. and Pandis, S. N.: An Algorithm for the Calculation of Secondary Organic Aerosol Density Combining AMS and SMPS Data, Aerosol Sci. Technol., 41(11), 1002–1010, doi:10.1080/02786820701666270, 2007.

Kroll, J. H., Chan, A. W. H., Ng, N. L., Flagan, R. C. and Seinfeld, J. H.: Reactions of Semivolatile Organics and their effects on Secondary Organic Aerosol Formation, Environ. Sci. Technol., 41, 3545–3550, doi:10.1021/es062059x, 2007.

Kroll, J. H., Donahue, N. M., Jimenez, J. L., Kessler, S. H., Canagaratna, M. R., Wilson, K. R., Altieri, K. E., Mazzoleni, L. R., Wozniak, A. S., Bluhm, H., Mysak, E. R., Smith, J. D., Kolb, C. E. and Worsnop, D. R.: Carbon oxidation state as a metric for describing the chemistry of atmospheric organic aerosol., Nat. Chem., 3(2), 133–9, doi:10.1038/nchem.948, 2011.

Kroll, J. H. and Seinfeld, J. H.: Chemistry of secondary organic aerosol: Formation and evolution of low-volatility organics in the atmosphere, Atmos. Environ., 42(16), 3593–3624, doi:10.1016/j.atmosenv.2008.01.003, 2008.

Kroll, J. H., Smith, J. D., Che, D. L., Kessler, S. H., Worsnop, D. R. and Wilson, K. R.: Measurement of fragmentation and functionalization pathways in the heterogeneous oxidation of oxidized organic aerosol, Phys. Chem. Chem. Phys., 11(Physical Chemistry of Aerosols), 8005–8014, 2009.

Lathem, T. L., Beyersdorf, A. J., Thornhill, K. L., Winstead, E. L., Cubison, M. J., Hecobian, A. H., Jimenez, J. L., Weber, R. J., Anderson, B. E. and Nenes, A.: Analysis of CCN activity of Arctic aerosol and Canadian biomass burning during summer, Atmos. Chem. Phys., 13, 2735–2756, doi:10.5194/acp-13-2735-2013, 2013.

Lee, B. H., Kostenidou, E., Hildebrandt, L., Riipinen, I., Engelhart, G. J., Mohr, C., DeCarlo, P. F., Mihalopoulos, N., Prevot, a. S. H., Baltensperger, U. and Pandis, S. N.: Measurement of the ambient organic aerosol volatility distribution: application during the Finokalia Aerosol Measurement Experiment (FAME-2008), Atmos. Chem. Phys., 10(24), 12149–12160, doi:10.5194/acp-10-12149-2010, 2010.

Lee, B.-H. and Pandis, S. N.: Volatility of atmospheric organic aerosol, Carnegie Mellon University, Pittsburgh., 2010.

Massoli, P., Lambe, a. T., Ahern, a. T., Williams, L. R., Ehn, M., Mikkilä, J., Canagaratna, M. R., Brune, W. H., Onasch, T. B., Jayne, J. T., Petäjä, T., Kulmala, M., Laaksonen, a., Kolb, C. E., Davidovits, P. and Worsnop, D. R.: Relationship between aerosol oxidation level and hygroscopic properties of laboratory generated secondary organic aerosol (SOA) particles, Geophys. Res. Lett., 37(24), doi:10.1029/2010GL045258, 2010.

Matsunaga, A. and Ziemann, P. J.: Gas-Wall Partitioning of Organic Compounds in a Teflon Film Chamber and Potential Effects on Reaction Product and Aerosol Yield Measurements, Aerosol Sci. Technol., 44, 881–892, doi:10.1080/02786826.2010.501044, 2010.

Meyer, N. K., Duplissy, J., Gysel, M., Metzger, A., Dommen, J., Weingartner, E., Alfarra, M. R., Fletcher, C., Good, N., McFiggans, G., Jonsson, Å. M., Hallquist, M., Baltensperger, U. and Ristovski, Z. D.: Analysis of the hygroscopic and volatile properties of ammonium sulphate seeded and un-seeded SOA particles, Atmos. Chem. Phys., 9, 721–732, doi:10.5194/acpd-8-8629-2008, 2009.

Moore, R. H., Nenes, A. and Medina, J.: Scanning Mobility CCN Analysis—A Method for Fast Measurements of Size-Resolved CCN Distributions and Activation Kinetics, Aerosol Sci. Technol., 44(10), 861–871, doi:10.1080/02786826.2010.498715, 2010.

Pandis, S. N., Harley, R. A., Cass, G. R. and Seinfeld, J. H.: Secondary Organic Aerosol Formation And Transport, Atmos. Environ. Part A-General Top., 26 13), 2269–2282, doi:10.1016/0960-1686(92)90358-R, 1992.

Petters, M. D. and Kreidenweis, S. M.: A single parameter representation of hygroscopic growth and cloud condensation nucleus activity, Atmos. Chem. Phys., 7(8), 1961–1971, doi:10.5194/acp-7-1961-2007, 2007.

Poulain, L., Wu, Z., Petters, M. D., Wex, H., Hallbauer, E., Wehner, B., Massling, A., Kreidenweis, S. M. and Stratmann, F.: Towards closing the gap between hygroscopic growth and CCN activation for secondary organic aerosols – Part 3: Influence of the chemical composition on the hygroscopic properties and volatile fractions of aerosols, Atmos. Chem. Phys., 10, 3775–3785, doi:10.5194/acpd-9-16683-2009, 2010.

Riipinen, I., Pierce, J. R., Donahue, N. M. and Pandis, S. N.: Equilibration time scales of organic aerosol inside thermodenuders: Evaporation kinetics versus thermodynamics, Atmos. Environ., 44, 597–607, doi:10.1016/j.atmosenv.2009.11.022, 2010.

Sareen, N., Schwier, A. N., Lathem, T. L., Nenes, A. and McNeill, V. F.: Surfactants from the gas phase may promote cloud droplet formation., Proc. Natl. Acad. Sci. U. S. A., 110(8), 2723–8, doi:10.1073/pnas.1204838110, 2013.

Shrivastava, M. K., Zelenyuk, A., Imre, D., Easter, R. C., Beranek, J., Zaveri, R. A. and Fast, J. D.: Implications of low volatility SOA and gas-phase fragmentation reactions on SOA loadings and their spatial and temporal evolution in the atmosphere, J. Geophys. Res. Atmos., 118(8), 3328–3342, doi:10.1002/jgrd.50160, 2013.

Surratt, J. D., Murphy, S. M., Kroll, J. H., Ng, N. L., Hildebrandt, L., Sorooshian, A., Szmigielski, R., Vermeylen, R., Maenhaut, W., Claeys, M., Flagan, R. C. and Seinfeld, J. H.: Chemical Composition of Secondary Organic Aerosol Formed from the Photooxidation of Isoprene, J. Phys. Chem. A, 110, 9665–9690, 2006.

Tritscher, T., Dommen, J., DeCarlo, P. F., Gysel, M., Barmet, P. B., Praplan, a. P., Weingartner, E., Prévôt, a. S. H., Riipinen, I., Donahue, N. M. and Baltensperger, U.: Volatility and hygroscopicity of aging secondary organic aerosol in a smog chamber, Atmos. Chem. Phys., 11(22), 11477–11496, doi:10.5194/acp-11-11477-2011, 2011.

Volkamer, R., Jimenez, J. L., San Martini, F., Dzepina, K., Zhang, Q., Salcedo, D., Molina, L. T., Worsnop, D. R. and Molina, M. J.: Secondary organic aerosol formation from anthropogenic air pollution: Rapid and higher than expected, Geophys. Res. Lett., 33, doi:10.1029/2006GL026899, 2006.

Vutukuru, S., Griffin, R. J. and Dabdub, D.: Simulation and analysis of secondary organic aerosol dynamics in the South Coast Air Basin of California, J. Geophys. Res., 111(D10), doi:D10s12 Artn d10s12, 2006.

Zhang, Q., Jimenez, J. L., Canagaratna, M. R., Allan, J. D., Coe, H., Ulbrich, I., Alfarra, M. R., Takami, A., Middlebrook, A. M., Sun, Y. L., Dzepina, K., Dunlea, E., Docherty, K., DeCarlo, P. F., Salcedo, D., Onasch, T., Jayne, J. T., Miyoshi, T., Shimono, A., Hatakeyama, S., Takegawa, N., Kondo, Y., Schneider, J., Drewnick, F., Borrmann, S., Weimer, S., Demerjian, K., Williams, P., Bower, K., Bahreini, R., Cottrell, L., Griffin, R. J., Rautiainen, J., Sun, J. Y., Zhang, Y. M. and Worsnop, D. R.: Ubiquity and dominance of oxygenated species in organic aerosols in anthropogenically-influenced Northern Hemisphere midlatitudes, Geophys. Res. Lett., 34(13), L13801, doi:10.1029/2007gl029979, 2007.

Table 1. Experimental Conditions

Expt. #	Seeds [a]	$[Toluene]_0$ [b] (ppb)	$[Toluene]_f$ [c] (ppb)	HONO injections	Lights (%)	[OH] exposure [d] (cm^{-3} s)
1	Yes	~ 300	na	1	~~30~~33	na
2	No	~ 200	na	1+1	100	na
3	Yes	~ 300	na	1+1	100	na
4	No	~ 200	na	2	100	na
5	Yes	~ 100	na	2+1	100	na
6	No	~ 100 [e]	na	2	100	na
7	Yes	1320	1130	1	~~100~~33	3.1×10^{10}
8	Yes	91 [g]	51 [h]	1	100	10×10^{10}
9	Yes	115	28	3+3	100	24×10^{10}

[a] $(NH_4)_2SO_4$ seed particles were used in some experiments

[b] Initial toluene concentrations estimated based on volume of VOC injected for Expts. 1-6 and measured by PTR-MS for Expts. 7-9

[c] Final toluene concentration after OH exposure

[d] Total OH exposure over the course of the experiment, estimated from exponential fits to the decay of toluene. Data not available for experiments 1-6 due to lack of PTR-MS data.

[e] Also injected 5 µl of benzene, o-xylene and 1,2,4-trimethylbenzene

[g] Also injected 16 ppb ethylbenzene, 12 ppb benzene and 23 ppb 1,2,4-trimethylbenzene

[h] Final concentrations of ethylbenzene, benzene and 1,2,4-trimethylbenzene: 9 ppb, 7 ppb and 13 ppb, respectively

Table 2. Summary of organic aerosol composition and volatility

Expt #	$(NO+NO_2)/OA$ [a]	OS_c [b]	O:C	NO^+/NO_2^+ [c]	$H_2O/(CO_2+{}^{13}CO_2)$	$^{13}CO/^{13}CO_2$ [c]	Volatility Reduction (25s) [e]	Volatility Reduction (15s) [e]
1	0.10	- 0.14	0.84	8.2	1.70	1.17	3.5	3.6
2	0.11	0.16	0.83	7.5	0.30	1.09	30.4	30.8
3	0.10	0.00	1.04	8.3	2.35	1.23	3.1	3.6
4	0.12	0.01	0.92	7.9	1.70	1.22	3.5	4.0
5	0.12	- 0.14	0.94	8.0	2.10	1.22	1.9	2.2
6	0.10	- 0.17	0.89	8.6	1.99	1.36	1.7	2.5
7	0.13	- 0.29	0.76	8.2	1.85	n/a[d]	1.0	1.0
8	0.10	- 0.05	0.94	7.3	1.67	1.13	4.3	4.9
9	0.12	- 0.04	1.02	7.0	2.40	1.13	6.2	8.2

[a] After first period of lights on. OA includes ~~the sum (~~NO^+ and NO_2^+~~)~~.

[b] After first period of lights on, OS_c approximated as $2\times$O:C - H:C.

[c] From linear regressions throughout the experiment (when OA present).

[d] Not applicable (no isotopically labeled VOC used in experiment 7)

[e] Volatility reduction estimated for data collected at residence times of 15 s and 25 s. Values are calculated relative to experiment 7 which featured the highest volatility.

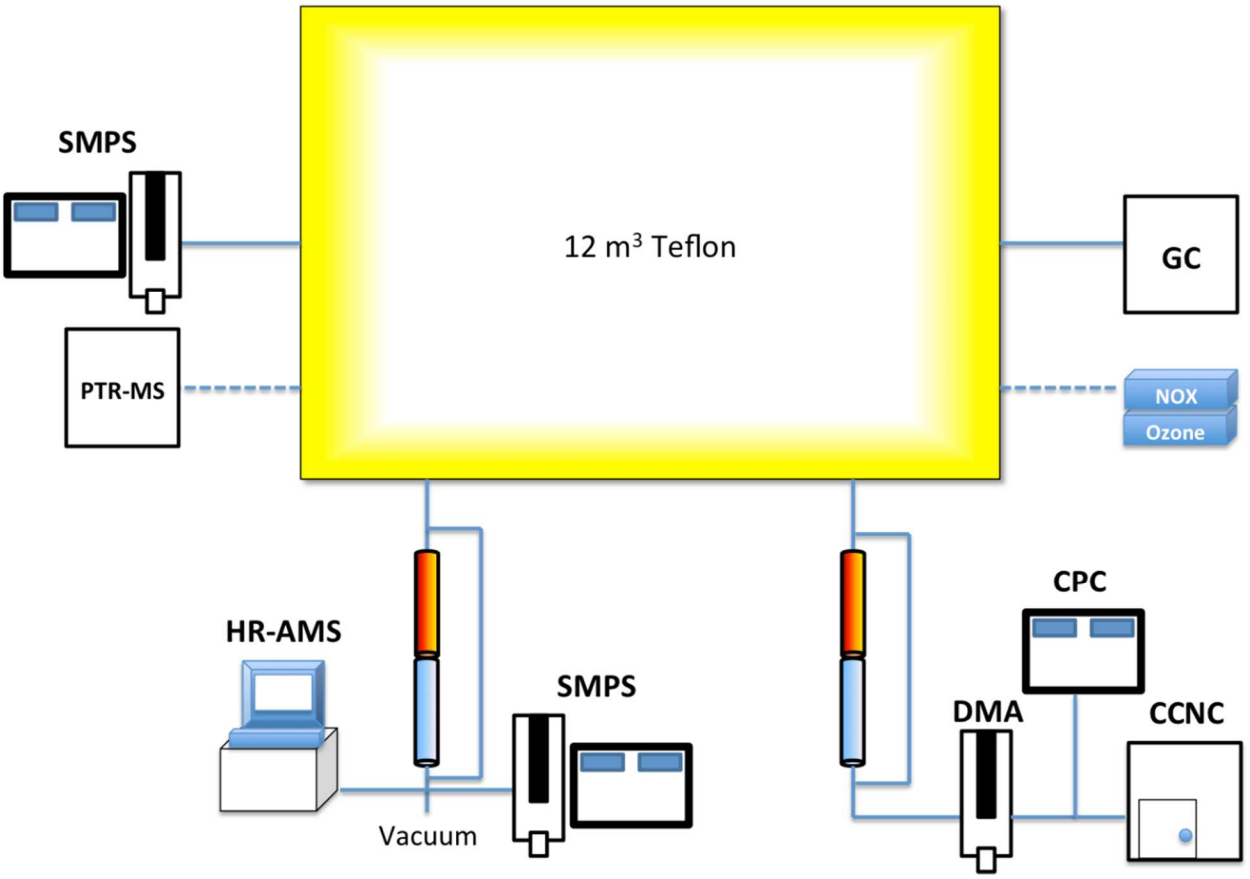

Figure 1. Schematic of experimental set-up. Dotted lines indicate that the equipment was used in selected experiments.

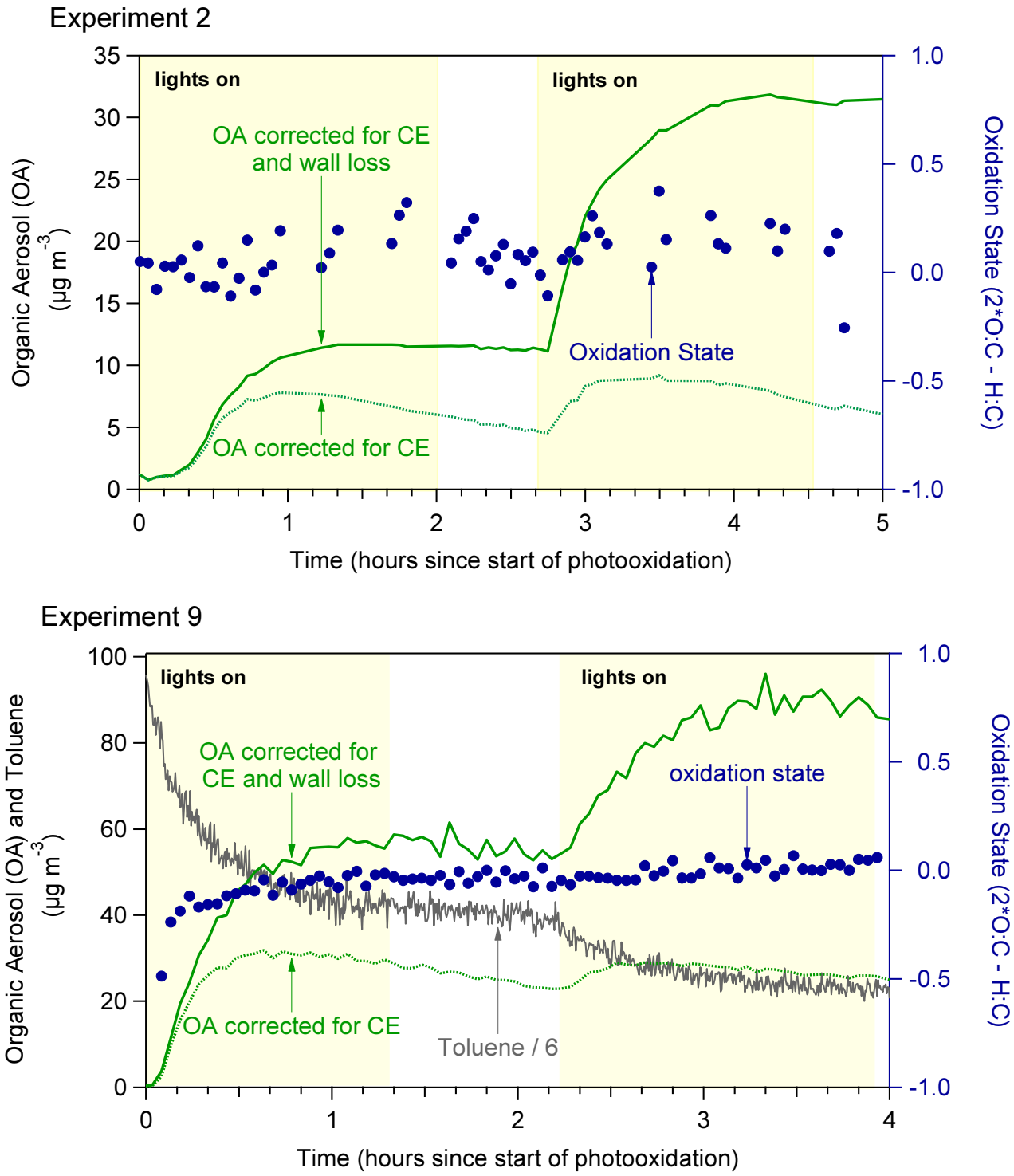

Figure 2. Time series of OA concentration (corrected for CE and corrected for CE and wall loss) from an unseeded experiment (2, top) and a seeded experiment (9, bottom), both with two photo-oxidation periods ("lights on") before which HONO was injected. The periods during which the

reactor was dark are shown with white background while the periods with UV-lights are shaded yellow. Also shown is the OA oxidation state (right axis) and concentrations of toluene during Expt. 9 (toluene concentrations have been divided by 6 on the figure for easier readability).

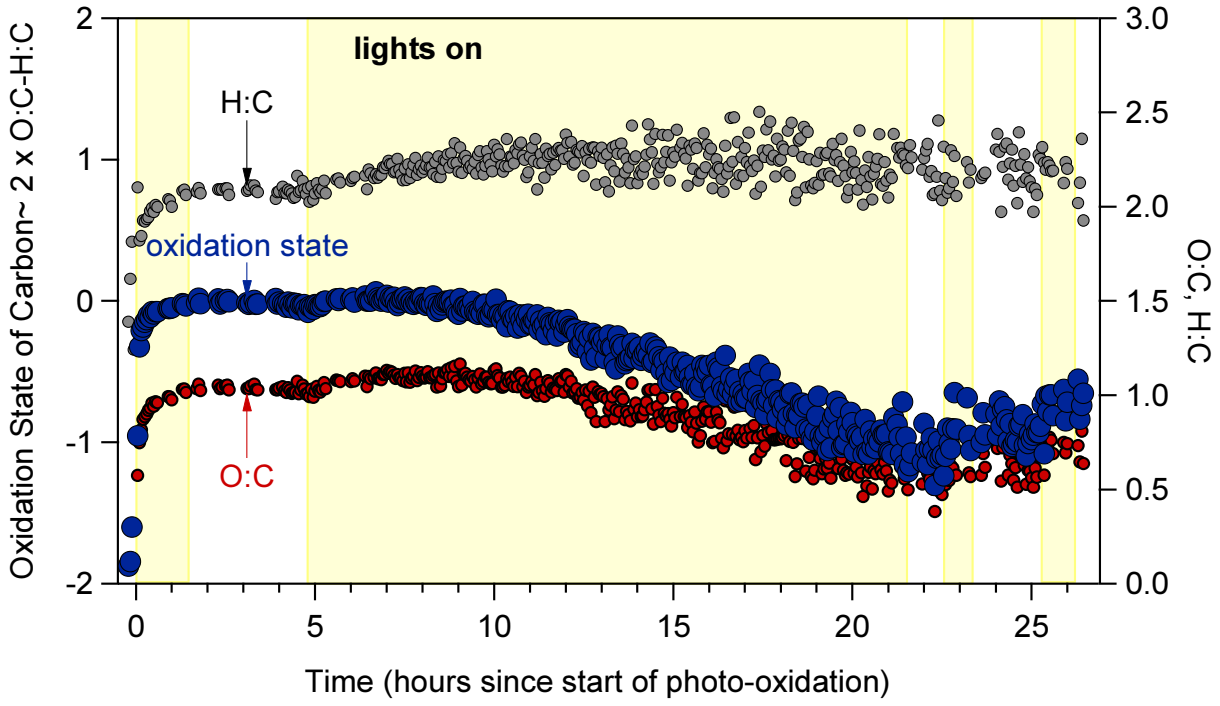

Figure 3. Time series of carbon oxidation state (left axis) and elemental ratios of O:C and H:C (right axis) for Expt. 3. The periods during which the reactor was dark are shown in with white background while the periods with UV-lights are shaded yellow.

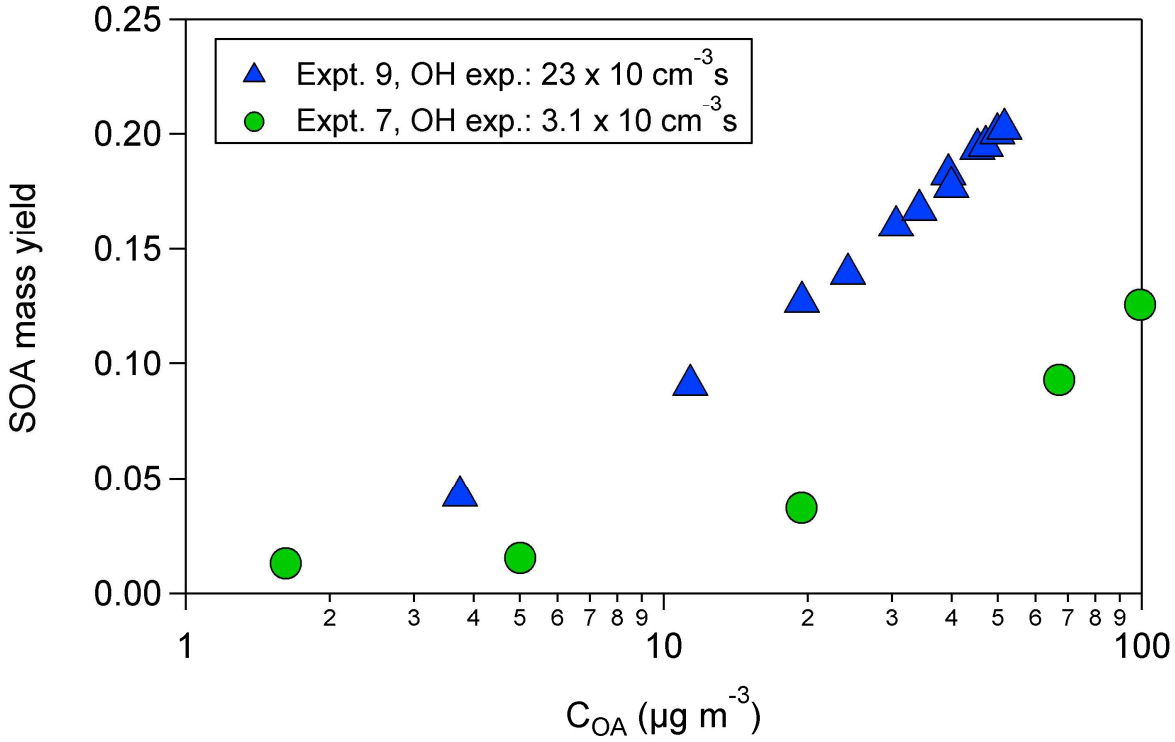

Figure 4. Organic aerosol mass yields for Expts. 7 and 9.

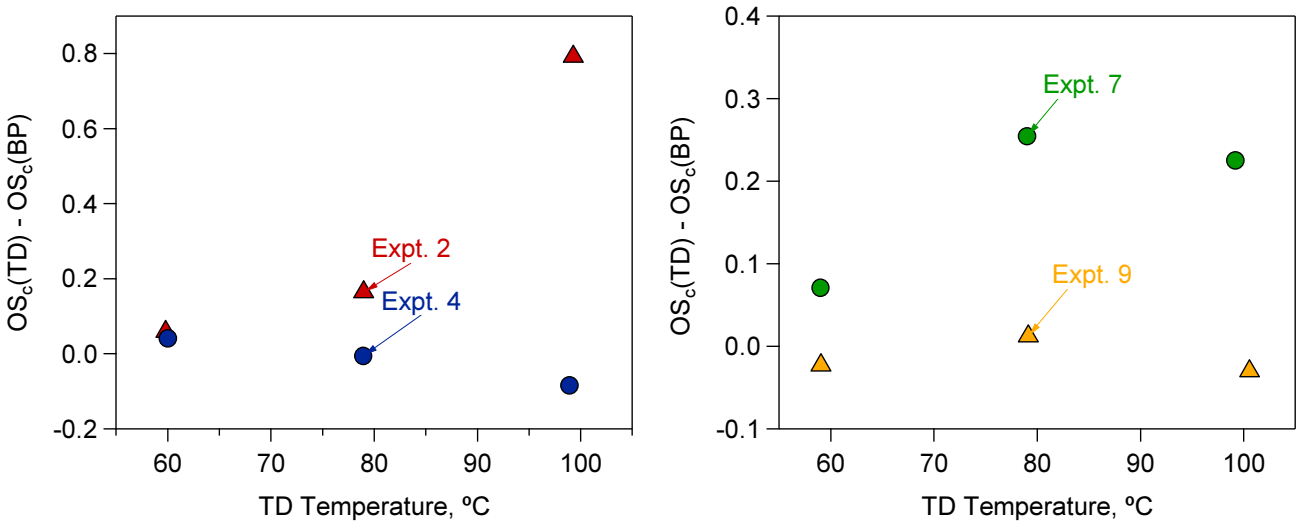

Figure 5. Comparison of the difference in oxidation state of denuded and total OA versus TD temperature for two unseeded experiments (2 and 4, left panel) and two seeded experiments (7 and 9, right panel). For OA of intermediate oxidation state (around 0, Expts. 4 and 9), oxidation state of the denuded OA is similar to the oxidation state of the full OA, implying that oxidation state does not correlate significantly with volatility. For OA of higher or lower oxidation state (Expts. 2 and 7, respectively) oxidation state anti-correlates with volatility, shown here as an increase in oxidation state difference with TD temperature.

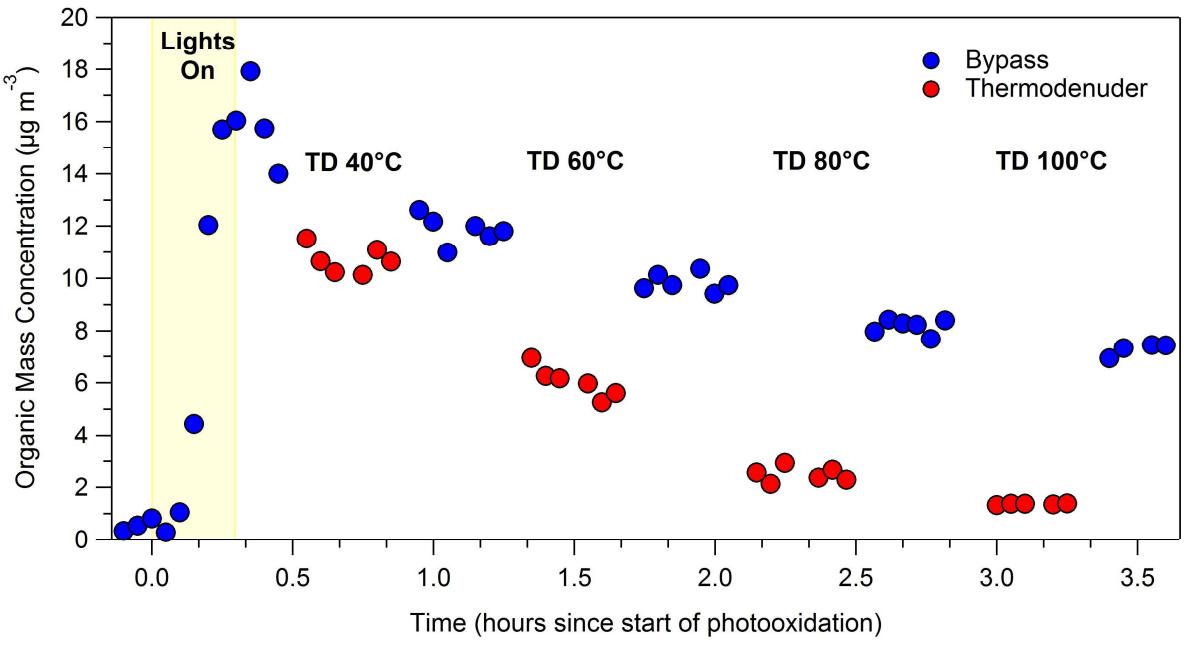

Figure 6. Bypass (blue) and thermodenuder (red) organic mass concentration time series for Expt. 7. The yellow shaded region denotes time when the UV lights were on. Temperatures represent the TD setpoint temperature. The bypass data have not been corrected for losses to the walls of the chamber. The TD measurements have not been corrected for losses in the TD.

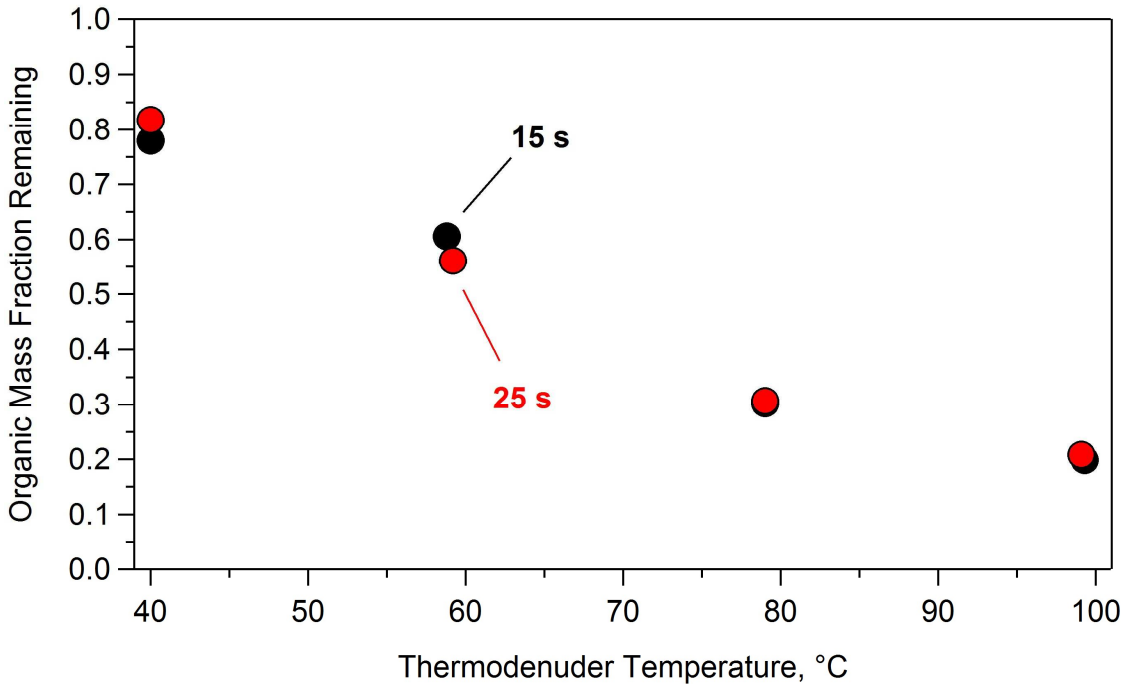

Figure 7. Organic mass fraction remaining as a function of thermodenuder temperature at a residence time of 15 s (black) and 25 s (red) for Expt. 7. Thermograms have been corrected for TD losses.

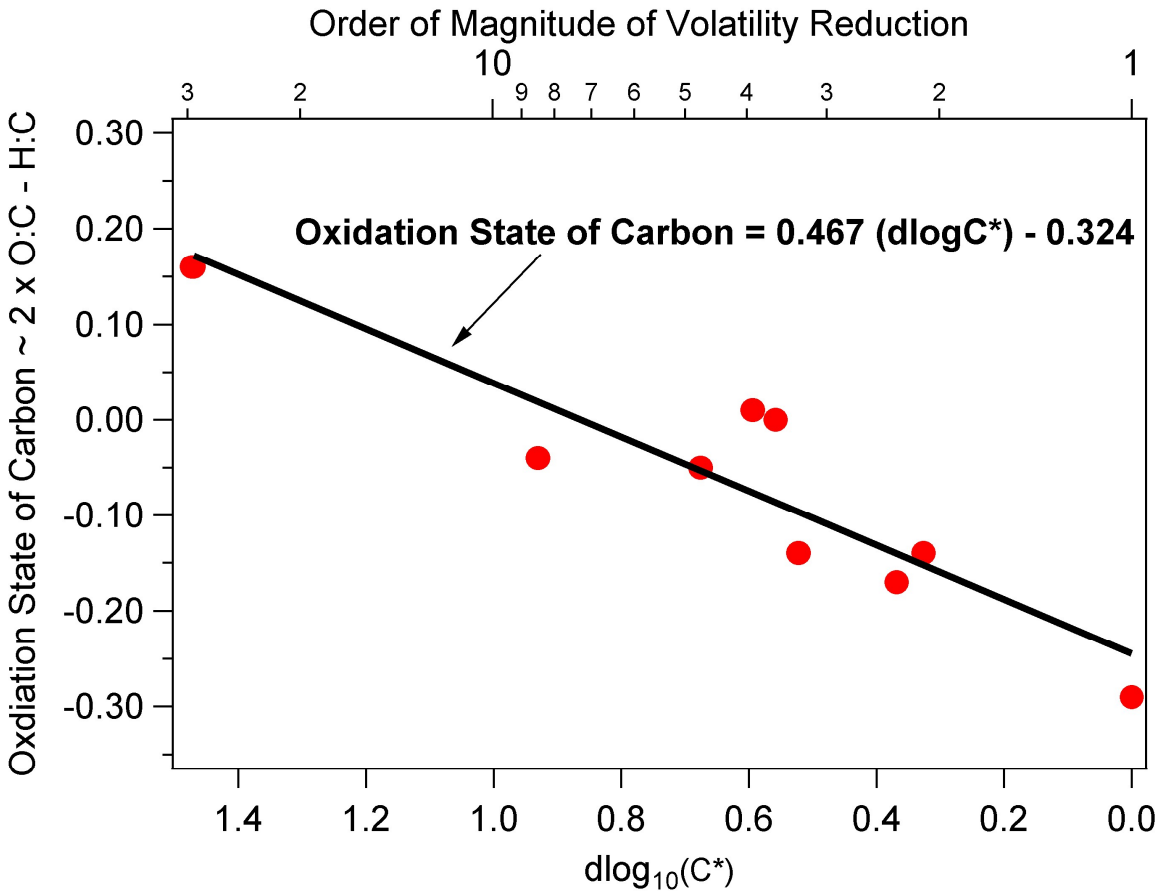

Figure ~~98~~. Oxidation state and volatility reduction in terms of change of log C* for the toluene SOA system. Red circles represent a single experiment and a single best-fit (black) line shows the trend.

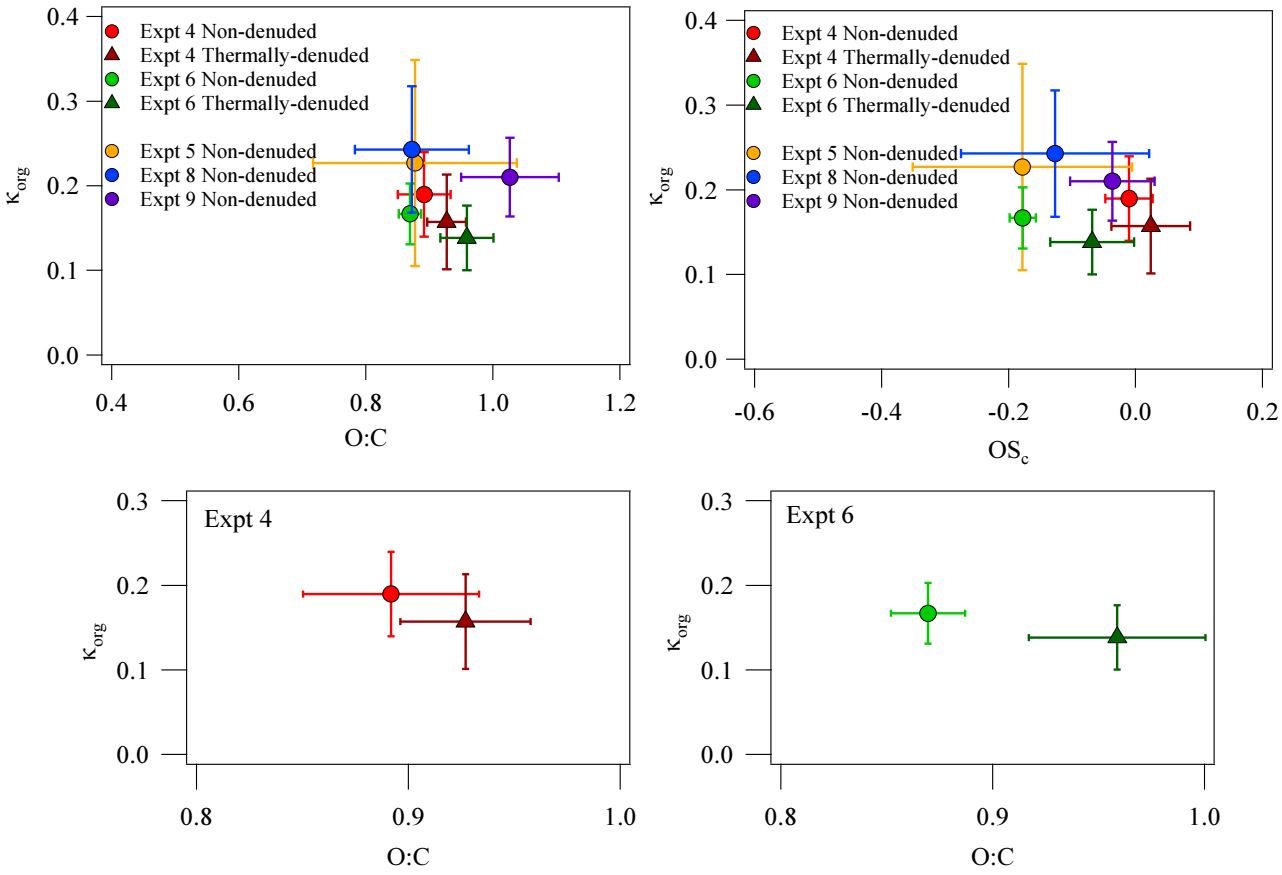

Figure 9~~10~~. κ_{org} versus O:C (top, left) and OS_c (top, right) for all experiments as listed in Table 1. Also shown are magnified hygroscopicity and O:C for unseeded experiments with non-denuded and thermally-denuded measurements (bottom). Vertical and horizontal error bars represent the standard deviation in κ_{org} and O:C or OS_c, respectively.